Threshold phenomena and bound states in the polaron problem

I. B. Levinson and É. I. Rashba

L. D. Landau Institute of Theoretical Physics, USSR Academy of Sciences

Usp. Fiz. Nauk **111**, 683–718 (December 1973)

A review is presented of theoretical and experimental studies that have established the possible existence of bound states of an electron or an exciton with an optical phonon (in semiconductors and ionic crystals). These states arise near a threshold, above which emission of an optical phonon is possible. The distinguishing features of bound states in which optical phonons participate is that they are nonconserved particles. The stability of the bound states is therefore due to the fact that their decay is forbidden by the energy and momentum conservation laws. Unlike virtual phonons of the polaron "jacket," the phonon in a bound state is "almost real." The onset of bound states is aided by strong electron-phonon interactions, by a strong magnetic field, by the large mass of the particle that is bound to the phonon, and by the small dispersion of the phonons. A position intermediate between bound states and ordinary polarons is occupied by hybrid states that are produced when the phonon energy coincides with one of the transition energies in the phononless system; in these states, the difference between the "real" and "virtual" phonons is lost. The existence of bound and hybrid states becomes manifest in a number of physical phenomena, primarily in optical effects.

CONTENTS

INTRODUCTION

Research on the polaron effect in semiconductors was devoted for a long time mainly to states close to the ground energy level ϵ_0 of the system. Calculations were made of the lowering of the ground-state level of the system as a result of electron-phonon interaction, of the renormalization of the effective masses of the electrons and excitons, of the polaron mobility, etc. The present status of the research in this direction is reflected in the review[1].

At the same time, the character of states with energy greatly exceeding ϵ_0 has remained little investigated until recently. This is due both to the specific difficulties that arise in the theory and to the fact that for a long time the available experimental data provided no stimulus for a detailed theoretical study of any definite section of the spectrum of the excited states.

Yet, from general theoretical considerations, which will be discussed later on, one should expect the appearance of characteristic singularities in the electron spectrum at energies close to the optical-phonon emission threshold. If the dispersion of the optical phonons can be neglected, as will be assumed from now on, then this threshold is located at $\epsilon_0 + \omega_0$, where ω_0 is the phonon frequency. Therefore during the last six years, when independent experiments were reported in which singularities were observed near $\epsilon_0 + \omega_0$ in the spectra of magnetopolarons[2,3], excitons[4], and impurity centers[5], the situation has changed radically. The near-threshold singularities have become in recent years the principal objects of investigation, and it is precisely in this region that the most interesting results were obtained.

The simplest argument favoring the assumption that the spectrum can have a complicated structure near the energy $\epsilon_0 + \omega_0$ consists in the following. When the system energy is somewhat higher than $\epsilon_0 + \omega_0$, there can exist in the system, independently, an electron subsystem (say a polaron), with an energy close to ϵ_0, and a "real" phonon. It is therefore natural that states that are produced somewhat lower than the threshold can constitute weakly bound states of a phonon with an electron. It suffices here, for example, to draw the analogy with the Wannier-Mott exciton.

In addition, there are general theoretical grounds for the appearance of singularities near $\epsilon_0 + \omega_0$, not connected in any way with particular models. In fact, it is well known[6] that the quantum-mechanical cross sections have singularities near reaction thresholds, and reactions with phonon production are now exceptions. To the contrary, inasmuch as the dispersion of the optical phonons is small, the threshold singularities in the electron mass operator $\mathcal{M}$ are enhanced, and this can result in a complete restructuring of the spectrum near the threshold.

Obviously, neglect of the optical-phonon dispersion is justified only if phonons with small momenta play the essential role. Then the theory pertains, strictly speaking, only to large-radius electronic states, which are described by the continual model. One can hope, however, that certain qualitative results of the theory remain in force also for systems that do not belong to this class.

The first theoretical investigations of threshold singularities were based on the single-phonon model, in which only phononless and single-phonon states were

taken into account. With the aid of this model it was possible to explain the cyclotron-resonance singularities that occur at $\omega_c \approx \omega_0$ (ω_c is the cyclotron frequency[7-9], to predict the existence of a new type of local oscillations near impurity centers[10], and also to justify the assumption that exciton-phonon complexes exist in the intermediate coupling[11].

It was observed at the same time that near the threshold $\epsilon_0 + \omega_0$, even in the case of weak electron-phonon coupling, there exist in certain cases complexes, namely states with an appreciable contribution of single-phonon states, i.e., with an appreciable average number $\langle N \rangle$ of phonons. We recall for comparison that near the bottom of the spectrum ϵ_0, the number of phonons in the polaron "jacket" we have $\langle N \rangle \sim \alpha$, where α is the coupling constant. Among the complexes, we can distinguish between hybrid states, in which the contributions of the single-phonon and phononless states are close, i.e., $\langle N \rangle \approx 1/2$, and bound states, in which the contribution single-phonon states predominates, i.e., $\langle N \rangle \approx 1$. Unlike the "proper polaron" state (as well as magnetopolaron or exciton states etc.) containing a small number of "virtual" phonons, bound states contain one "almost real" phonon. Of course, from the general theoretical point of view, the complexes can be regarded simply as definite branches of the polaron spectrum. The properties, however, are so unique that it is more convenient to regard them as a separate group of states.

The single-phonon model is most suitable for the description of the resonant situation, when one of the excitation energies of the electron subsystem is close to ω_0 (Fig. 1a). This situation can arise either when the electron system has a discrete spectrum (electron in an impurity center), or when it has in addition to the continuous spectrum also discrete quantum numbers (Landau electron, magnetoelectron), which also ensures the presence of discrete frequencies. Obviously, the presence of a resonance enhances the electron-phonon interaction effect. A typical result obtained with the aid of the single-phonon model is that near the threshold there are no more than two levels, in accordance with the number of states taken into account in this model.

Further development of the theory has shown that the spectrum near the threshold can actually be much richer and can contain an infinite series of bound states that condense towards the threshold. The existence of such states is not connected in any way with resonance, and can take place in the situations illustrated in Fig. 1c.

These states were first observed for the polaron in the limit of the adiabatic strong electron-phonon coupling[12], where the single-phonon model is known to be inapplicable. In these states, the number of "almost real" phonons is larger by one than for the polaron states near the bottom of the band. There are no such states for weak couplings[12,13].

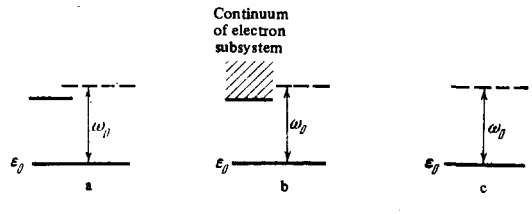

FIG. 1. Three situations that can arise near the optical-phonon emission threshold [18]. a) Resonant situation, with a discrete level of the electron subsystem near the threshold; b) the threshold falls in the continuum of the electron subsystem; c) the electron subsystem has no levels near the threshold.

A study of the corrections to the single-phonon model has shown that in a number of cases in the immediate vicinity of the threshold this model is inapplicable even in case of weak coupling[9,14]. The single-phonon model is equivalent to taking into account only the simplest diagram for the mass operator M. Yet near the threshold the diagrams of higher orders increase progressively and the perturbation-theory series for M diverges. To find the spectrum in this region it is necessary to sum an infinite sequence of diagrams for M, or equivalently, solve an integral equation for the electron-phonon vertex Γ[15]. When this procedure was carried out explicitly for the magnetopolaron[16] it turned out that an infinite sequence of bound states of the electron and phonon can exist below the threshold even in the case of weak coupling.

We have assumed above and will assume throughout that the widths of the electron and exciton band exceed ω_0, as is the case in typical semiconductors. The formation of bound states is then closely connected with threshold phenomena. However, bound states (exciton plus phonon, exciton plus magnon, two phonons, etc.) arise also in systems where ω_0 exceeds the band width, namely in organic crystals, magnets, etc. A comparison of systems of both types is given in[17].

A distinguishing feature of complexes, including the optical phonon, is that a nonconserved particle takes part in them. Indeed, the Hamiltonian of the electron-phonon interaction is usually chosen to be linear in the phonon amplitudes, and consequently does not conserve the number of phonons. Therefore the stability of complexes with respect to decay with vanishing of a phonon is determined only by the energy and momentum conservation laws.

The general plan of the present review is the following. In Chap. 2 we consider the single-phonon model, and in Chap. 3 we present a general derivation of the equation for Γ in the case of weak coupling. In the succeeding chapters, the theory developed is applied to particular systems and the experimental data are discussed in passing[1]. In those cases when the weak coupling will do, the theory is based entirely on the general approach developed in Chaps. 2 and 3.

1. ELECTRON-PHONON INTERACTION

The traditional form of the electron-phonon interaction Hamiltonian is

$$\mathcal{H}_{eL} = \frac{1}{V^{1/2}} \sum_{\mathbf{q}} c_{\mathbf{q}} e^{i\mathbf{q}\mathbf{r}} b_{\mathbf{q}} + \text{э. с.}, \qquad (1.1)$$

where $\mathbf{r}$ is the electron coordinate, $\mathbf{q}$ is the phonon momentum, $b_{\mathbf{q}}$ is the phonon annihilation operator, $c_{\mathbf{q}}$ is the interaction matrix element, and V is the volume of the system. The final results usually contain the quantity

$$\mathcal{B}(\mathbf{q}) = |c_{\mathbf{q}}|^2, \qquad (1.2)$$

which depends in the isotropic case only on the modulus of $\mathbf{q}$. For interaction with dispersionless optical phonons, this quantity is conveniently represented in the form

$$\mathcal{B}(q) = \alpha \frac{4\pi\omega_0^2}{p_0^3} \Phi(q), \quad p_0 = \sqrt{2m\omega_0}, \qquad (1.3)$$

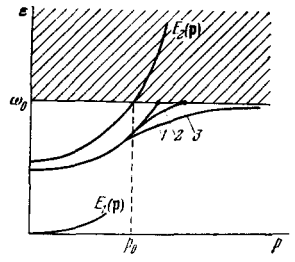

FIG. 2. Variation of spectrum in single-phonon model.

where α is a dimensionless coupling constant and m is the effective mass of the electron. The form factor

$\Phi(q)$ = 1—deformation interaction (DO interaction)
= p_0^2/q^2—polarization interaction (PO interaction).

For the PO interaction, the value of α defined in this manner coincides with the Froehlich value

$$\alpha=\frac{e^2}{v_0}\frac{1}{\bar{\varkappa}},\quad \frac{1}{\bar{\varkappa}}=\frac{1}{\varkappa_\infty}-\frac{1}{\varkappa_0},\quad \frac{1}{2}mv_0^2=\omega_0, \tag{1.5}$$

where κ_∞ and κ_0 are the high-frequency and low-frequency dielectric constants. A distinction is made between the cases of weak ($\alpha \ll 1$), intermediate ($\alpha \sim 1$), and strong ($\alpha \gg 1$) coupling.

Sometimes $\mathscr{H}_{eL}$ includes terms that are quadratic in b and b^+; so far, however, only the magnetopolaron problem was considered with this type of interaction (Chap. 7).

2. SINGLE-PHONON MODEL

We consider a simple model in which a particle with two branches of the bare spectrum $E_1(p)$ and $E_2(p)$ interact at zero temperature with optical phonons of frequency ω_0 (without dispersion), and the emission of a phonon transfers the particle from one branch to the other (Fig. 2). How does the upper branch 2 vary as a result of this interaction?

We assume first that the interaction with the phonons is weak. Then, in addition to the phononless states $\varphi_s(p)$ (particle with momentum p on branch s = 1, 2) it suffices to consider the single-phonon state $\varphi_s(p, q)$ (q is the phonon momentum). The perturbed wave function for branch 2 is

$$\psi_2(p)\infty\varphi_2(p)+\int\frac{d^3q}{(2\pi)^3}\frac{\gamma_{12}(q)}{\varepsilon-\omega_0-E_1(p-q)+i0}\varphi_1(p-q,q), \tag{2.1}$$

where $\gamma_{1,2}$ is the matrix element of the interaction (1.1), and the energy $\epsilon = \epsilon(p)$ should be determined from the equation

$$\varepsilon - E_2(p) = \mathscr{M}^0(\varepsilon p), \tag{2.2}$$

where

$$\mathscr{M}^0(\varepsilon p)=\int\frac{d^3q}{(2\pi)^3}\frac{|\gamma_{12}(q)|^2}{\varepsilon-\omega_0-E_1(p-q)+i0}, \tag{2.3}$$

We assume, as usual, that $E_1(p)$ reaches a minimum at p = 0, and we put $E_1(0) \equiv \epsilon_0 = 0$. Then, if the energy ϵ is close to the threshold ω_0, then the denominator can become small (at $q \approx p$). This is precisely why the exact energy ϵ in the denominator is not replaced by the unperturbed energy $E_2(p)$, i.e., Wigner-Brillouin perturbation theory is used rather than Rayleigh-Schrödinger theory.

In the region above the threshold ($\epsilon > \omega_0$) there is no single-particle spectrum in the usual sense of the word, and there is only a continuous spectrum of decay states. We confine ourselves therefore for the time being to the region below the threshold ($\epsilon < \omega_0$). In this region, the probability of observing a phononless state φ_2 when the system is in the quantum state ψ_2 is

$$Z(p)=\left[1+\int\frac{d^3q}{(2\pi)^3}\left|\frac{\gamma_{12}(q)}{\varepsilon-\omega_0-E_1(p-q)}\right|^2\right]^{-1}_{\varepsilon=\varepsilon(p)}=\left[1-\frac{\partial}{\partial\varepsilon}\mathscr{M}^0(\varepsilon p)\right]^{-1}_{\varepsilon=\varepsilon(p)}. \tag{2.4}$$

In other words, the effective number of phonons participating in the production of ψ_2 is $\langle N \rangle = 1 - Z$.

Since the denominator in $\mathscr{M}^0$ can vanish, starting with $\epsilon = \omega_0$, the quantity $\mathscr{M}^0$ as a function of ϵ becomes nonanalytic as $\epsilon \to \omega_0$. The character of this nonanalyticity is determined by the behavior of the integrand at values of q close to p. It follows therefore that the behavior of $\mathscr{M}^0(\epsilon)$ near the threshold is determined by the behavior of $E_1(p)$ at $p \approx 0$, i.e., by the spectrum at the bottom to which the particle collapses after emitting the phonon, and the behavior of $\gamma_{12}(q)$ at $q \approx p$, i.e., the interaction with that phonon to which the particle transfers its momentum.

In a number of cases it is convenient to use a somewhat modified formulation of the problem, in which we are interested in a definite state of branch 2 (e.g., p = 0), but this state can be controlled with the aid of an external parameter, say a magnetic field H. Then E_2 and $\mathscr{M}^0$ will depend not on p but on H. Since E_2 usually increases monotonically with increasing H as well as with increasing p, everything said henceforth concerning the dependence of the spectrum on p pertains equally well to the dependence of the spectrum on H or on some other external parameter.

If ϵ is far from the threshold, then the right-hand side of (2.2) is certainly small and, substituting $\epsilon = E_2$, we obtain the usual polaron renormalization of the spectrum, which is small in the weak-coupling case considered here. This situation takes place in the initial segment of the branch 2. On this segment $Z(p) \approx 1$, i.e., the states are practically phononless.

When the momentum approaches p_0, the energy ϵ approaches ω_0, and the subsequent behavior of the spectrum depends essentially on the character of the nonanalyticity of $\mathscr{M}^0(\epsilon)$ [15]. We note that if one studies the dependence of the spectrum on an external parameter, then the approach to the threshold means an approach to resonance between the frequency of the phonon ω_0 and the frequency of the transition in the spectrum $E_2 - E_1$. In these cases, the threshold effects become resonant.

Let us examine now several characteristic types of nonanalyticity arising in real problems (Table I):

a) $\mathscr{M}^0(\varepsilon) = -A + B(\omega_0 - \varepsilon) - C(\omega_0 - \varepsilon)^{3/2} + \ldots$, (2.5a)
b) $\mathscr{M}^0(\varepsilon) = -A + B(\omega_0 - \varepsilon)^{1/2} + \ldots$, (2.5b)
c) $\mathscr{M}^0(\varepsilon) = -A(\omega_0 - \varepsilon)^{-1/2} + \ldots$, (2.5c)
d) $\mathscr{M}^0(\varepsilon) = -A(\omega_0 - \varepsilon)^{-1} + \ldots$ (2.5d)

The quantities A, B, C in these equations are real; they can be regarded as independent of p or H, since this dependence usually does not affect the picture of the spectrum near the threshold. Cases (a)—(c) correspond to the dispersion laws shown in Fig. 2 by curves 1—3, respectively.

In the case of strong nonanalyticity (curve 3), the spectrum continues without limit into the region of large momenta, and the energy ceases in practice to

TABLE I. Classification of threshold phenomena by the character of the nonanalyticity.

Character of nonanalyticity	Branches of spectrum	Physical object 1	Physical object 2	Parameter controlling the spectrum	Reference
a	Exciton (interacting with polarization phonons)	Exciton level 1s	Levels $2s, 3s, \ldots$	Position of level 2 relative to level 1	11, 18
b	Ditto	Ditto	Levels $2p, 3p, \ldots$	Ditto	11, 18
c	Electron	Polaron branch		Momentum	19
b	Exciton in strong magnetic field	Exciton under lowest Landau band n = 0.	Exciton under Landau band n = 1	Magnetic field	20
c	Electron in strong magnetic field	Electron in lowest Landau band n = 0	Electron in any Landau band n=0,1, ...whose bottom is lower than ω_0	Longitudinal momentum component	21, 22
			Electron in Landau band n = 1	Magnetic field	2, 8, 9
c	Electron at p = 0 (interacting with polarization phonons).	Polaron branch		None	12
c	Exciton in one-dimensional crystal	Exciton branch		Momentum	23
d	Impurity center	Electronic ground level	Excited level	Distance between levels	10

depend on p and is approximately equal to ω_0. This phenomenon has been named pinning; one speaks of the pinning of branch 2 to the branch 1 + phonon. We consider now the structure of the states in the pinning region, i.e., as $\epsilon \to \omega_0$. It is easily seen that in this case $Z \to 0$, i.e., the bare states φ_2 take practically no part in the formation of these states. The main contribution to the integration with respect to q in (2.3) is made by the region where $E_1 \approx 0$. This means that in the pinning region the particle is at the bottom of band 1, and therefore the energy and momentum of the state in the pinning region are due practically entirely to the phonon. The difference between the total energy ω_0 of the particle and the phonon and the energy of these states can be interpreted as the binding energy. From this point of view, the states in the pinning region are bound states of the particle at the bottom of band 1 and the phonon.

States with momenta close to p_0 are intermediate between polaron states at the start of the branch and bound states at the end of the branch. It is easy to verify that for these states we have $Z(p_0) \approx 1/2$, i.e., these states contain phononless and single-phonon states in equal amounts. We shall call states of this type hybrid. In both hybrid and bound states there is a noticeable participation of an almost "real" phonon. It is therefore convenient to combine them into a common concept—"particle + phonon" complex.

If we put $A = \alpha\omega_0^{3/2}$ in (2.5c), then α plays the role of a dimensionless coupling constant. We can then show that the hybrid states lie at a distance $|\epsilon - \omega_0| \sim \alpha^{2/3}\omega_0$ from the threshold, and the bound states for which $Z \ll 1$ lie at a distance $|\epsilon - \omega_0| \ll \alpha^{2/3}\omega_0$. Thus, with increasing momentum we pass successively through polaron states with $\langle N \rangle \sim \alpha$, hybrid states with $\langle N \rangle \approx 1/2$, and bound states with $\langle N \rangle \approx 1$.

In case (b) with the weaker nonanalyticity, the spectrum has an end point and approaches this end point tangent to the straight line $\epsilon = \omega_0$, i.e., we likewise have pinning, but less pronounced. Obviously, $Z \to 0$ as $\epsilon \to \omega_0$, so that near the threshold we have again bound states, and hybrid states are located between the bound states and the start of the branch. If we put $B = \alpha\omega_0^{1/2}$ in (2.5b), then the hybrid states are located at a distance $|\epsilon - \omega_0| \sim \alpha^2\omega_0$ from the threshold, and the bound states at a distance $|\epsilon - \omega_0| \ll \alpha^2\omega_0$. In the real situation, the threshold is always smeared out and if its smearing is not too small, then cases (b) and (c) are qualitatively close, since the farther part of branch 3 falls in the smearing region and does not come into play.

Very weak nonanalyticity corresponds to the case (a). The spectrum has an end point which it approaches with a finite slope. Obviously, $Z \approx 1$ everywhere, even in the immediate vicinity of the threshold, i.e., there are no hybrid states, and all the more no bound states below the threshold in this case.

The possibility of introducing quasiparticles in the region of the continuous spectrum near the threshold is also connected with the degree of nonanalyticity. In cases (a) and (b), when the spectrum has an end point, this is possible, since the reciprocal lifetime of the quasiparticle $\Gamma(\epsilon) = \mathrm{Im}\,\mathcal{M}^0(\epsilon) \to 0$ as $\epsilon \to \omega_0$. In case (c) we have $\Gamma(\epsilon) \to \infty$ as $\epsilon \to \omega_0$, and therefore there are no quasiparticles directly beyond the threshold. We note also that owing to the interaction with the phonons the bottom of branch 1 shifts downward; this leads to a renormalization of the position of the threshold, but does not influence the qualitative picture of the spectrum.

Case (d), corresponding to impurity centers, occupies a somewhat singular position. Neither E_1 nor E_2 depends on p; since the spectrum is discrete, there is no continuum at $\epsilon > \omega_0$, and undamped states exist both below and above the threshold (Fig. 3). In this case there is likewise pinning as a function of the position of the level E_2 relative to $E_1 = 0$.

3. THRESHOLD APPROXIMATION

The quantity $\mathcal{M}^0$ defined by formula (2.3) is a mass operator calculated in the lowest order in the interac-

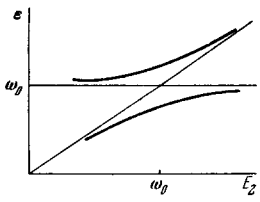

FIG. 3. Variation of impurity-center spectrum in interaction with optical phonons; it is assumed that $E_1 = 0$.

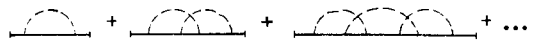

FIG. 4. Sequence of electron-mass-operator diagrams, which plays an important role in the threshold approximation.

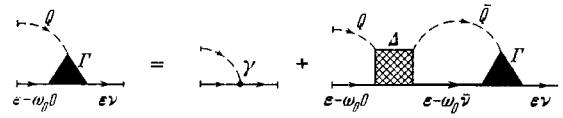

FIG. 5. Equation for the vertex.

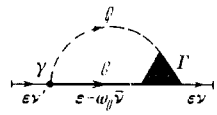

FIG. 6. Expression for the mass operator in terms of Γ.

tion (simplest diagram in Fig. 4). To estimate the limits of applicability of the single-phonon model it is necessary to calculate the contributions from the next higher orders of perturbation theory. Direct calculation shows that if $\mathcal{M}^0(\epsilon)$ increases without limit as $\epsilon \to \omega_0$ (cases (c) and (d)), then the contributions from the next higher orders increase even more rapidly as $\epsilon \to \omega_0$, and the rate of growth increases with the order of the contribution. The diagrams that are significant in circumstances of this type were separated by Pitaevskiĭ [15]; it was shown that the dangerous sections of the diagrams in the near-threshold region are those in which the decay process is almost real. Near the threshold with emission of an optical phonon, the dangerous sections are those along one electron and one phonon line. The separation of the dangerous cross sections leads to an equation for the vertex Γ, which is shown for the considered case in Fig. 5. In this figure, the solid and dashed lines correspond to the Green's functions G and D of the electron and phonon, respectively; γ is the bare vertex determined from the Hamiltonian (1.1); the shaded rectangle Δ is compact, i.e., it has no dangerous sections. If we find Γ, then we can calculate $\mathcal{M}$ with the aid of the Dyson equation (Fig. 6).

It is assumed henceforth that the system is at zero temperature and that the electron concentration is vanishingly small. By virtue of the latter circumstance, we can neglect the renormalization of D in all the internal lines, and assume

$$D(\omega \mathbf{q}) = \frac{1}{\omega - \omega_0 + i0} - \frac{1}{\omega + \omega_0 - i0}. \tag{3.1}$$

For the same reason, all the G are retarded. This enables us to integrate with respect to the energy parameters ω[14] in all the diagrams, using the relation

$$\int_{-\infty}^{+\infty} \frac{d\omega}{2\pi} iD(\omega \mathbf{q}) F(\omega) = F(\omega_0 - i0), \tag{3.2}$$

where $F(\omega)$ is analytic at $\mathrm{Im}\,\omega < 0$. This means that in all G it is necessary to replace all the ω by ω_0, and that the internal phonon line corresponds only to integration with respect to q.

We consider first the representation of $\mathcal{M}$ shown in Fig. 6, where ν is the set of the quantum numbers of the electrons, ε is its energy parameter, and Q denotes the set of those phonon-momentum components q which are not determined from the quantum numbers of the electrons by the conservation laws at the vertex. Obviously,

$$\mathcal{M}_{\nu'\nu}(\varepsilon) = \int d\bar{\nu} \int dQ \gamma^*_{\nu'\bar{\nu}}(Q) G_{\bar{\nu}}(\varepsilon - \omega_0) \Gamma_{\bar{\nu}\nu}(\varepsilon; Q). \tag{3.3}$$

If ε lies near the threshold, then $\epsilon - \omega_0$ lies near the bottom of the spectrum, where perturbation theory is applicable. Therefore, if we are not interested in the renormalization of the threshold due to the renormalization of the bottom, then we can replace the energy G by the free energy:

$$G^0_{\bar{\nu}}(\varepsilon - \omega_0) = (\varepsilon - \omega_0 - E_{\bar{\nu}} + i0)^{-1}, \tag{3.4}$$

where $E_{\bar{\nu}}$ is the spectrum of the free electrons. Let $\nu = 0$ correspond to the ground state, and let again $E_0 = 0$. We then see that when ε is close to the threshold ω_0 the value of $G_{\bar{\nu}}$ as a function of $\bar{\nu}$ is large when $\bar{\nu}$ is close to zero. Under these conditions we can take γ and Γ outside the integral with respect to $\bar{\nu}$ at $\bar{\nu} = 0$. This actually means that we assume that the vertices are analytic in $\bar{\nu}$, an assumption that holds true in most cases of interest. For γ this can be verified directly, and for Γ this can be checked after Γ is determined. We can therefore write

$$\mathcal{M}_{\nu'\nu}(\varepsilon) = \Lambda(\varepsilon) \int dQ \gamma^*_{\nu' 0}(Q) \Gamma_{0\nu}(\varepsilon; Q), \tag{3.5}$$

where

$$\Lambda(\varepsilon) = \int d\nu G^0_{\nu}(\varepsilon - \omega_0). \tag{3.6}$$

Since $\mathcal{M}^0$ is obtained from $\mathcal{M}$ by replacing Γ by γ, we see therefore that $\Lambda(\epsilon)$ and $\mathcal{M}^0(\epsilon)$ exhibit an identical behavior as $\epsilon \to \omega_0$. It is also easily seen that the singularities of these quantities are connected with the behavior of the density of states $\rho(\epsilon)$ at the bottom of the spectrum since $\mathrm{Im}\,\Lambda(\epsilon) \propto \rho(\epsilon - \omega_0)$.

By exactly the same reasoning, we can transform the equation of Fig. 5 for the sought $\Gamma_{0\nu}$ into

$$\Gamma_{0\nu}(\varepsilon; Q) = \gamma_{0\nu}(Q) + \Lambda(\varepsilon) \int d\bar{Q} \Delta_{00}(\varepsilon; Q, \bar{Q}) \Gamma_{0\nu}(\varepsilon, \bar{Q}). \tag{3.7}$$

The quantity Δ has no dangerous cross sections and is therefore regular near the threshold; we can put for it $\epsilon = \omega_0$, and calculate it in the case of weak coupling by perturbation theory. If we confine ourselves to the simplest diagram for Δ, shown in Fig. 7, then the solution of (3.7) is equivalent, after substituting Γ in (3.5), to summation of the series shown in Fig. 4.

The derivation of (3.7) is in a certain sense schematic. Thus, it was assumed that the level $\nu = 0$ is not degenerate and that $\gamma_{0\nu}(\mathbf{Q})$ has no singularities. These limitations can be easily lifted by modifying the derivation for each particular case. For example, such a generalization was carried out in[13] for the case of a singularity in γ, as applied to a polaron with $p = 0$. The only important circumstance is that the integration is always carried out only with respect to those variables which do not influence the total energy of the electron and the phonon in the dangerous cross section.

Equation (3.7) is an integral equation for Γ with kernel Δ and with parameter Λ. Although the kernel is small, $\Delta \propto \gamma^2 \propto \alpha$, this smallness can be offset by the large value of Λ near the threshold. If Λ is bounded or

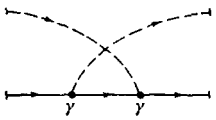

FIG. 7. Simplest approximation of the kernel of the equation for Γ.

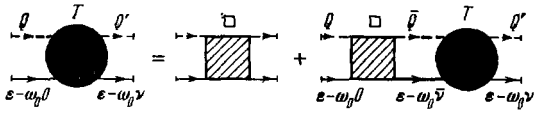

FIG. 8. Equation for the scattering amplitude T.

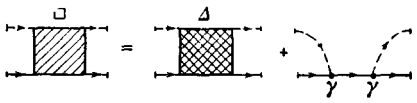

FIG. 9. Connection between the kernels of the equations for Γ and T.

if ϵ is sufficiently far from the threshold, then the equation can be iterated; this corresponds to expansion of $\mathscr{M}$ in powers of α. On the other hand, if Λ is not bounded and we are interested in the immediate vicinity of the threshold, then the equation must be solved without resorting to iteration.

This was done for the magnetopolaron[16] and for the impurity center[24]. In both cases there exists an infinite sequence of levels condensing to the threshold and describing bound states of the electron and phonon. The richness of the near-threshold energy spectrum is directly connected with the richness of the spectrum of the corresponding integral equation for Γ.

It is appropriate to note here that the equation used in[15] for Γ was algebraic and not integral, and therefore did not lead to a rich near-threshold spectrum. The integral character of the equation for Γ is connected with the fact that the optical phonon has a negligibly small dispersion. Therefore the energy in the dangerous section does not depend on Q, and states with all Q are near-threshold and the integration with respect to them is conserved.

The connection between the energy spectrum and the spectrum of the integral equation becomes most pronounced when the equation for the electron-phonon scattering amplitude T is considered (Fig. 8). This equation can be obtained literally in the same manner as the equation for Γ:

$$T_{0v}(\varepsilon;\ Q,\ Q') = \square_{0v}(Q,\ Q') + \Lambda(\varepsilon)\int d\bar{Q}\,\square_{00}(Q,\bar{Q})\,T_{0v}(\varepsilon;\bar{Q},Q'). \quad (3.8)$$

The kernel □ of this equation is connected with the kernel Δ of the equation for Γ by the relation of Fig. 9. It is seen from (3.8) that T is the resolvent of the kernel □; there T has a singularity when $\Lambda(\epsilon)$ coincides with one of the eigenvalues of the kernel Λ_Γ. This means that the equation

$$\Lambda(\varepsilon) = \Lambda_\Gamma \quad (3.9)$$

determines the spectrum of the two-particle bound states of the electron and phonon. It is appropriate to note here that since the phonon is a non-conserved quantity, the spectra of the single-phonon Green's function G and of the two-particle function K = KD + GDTGD coincide[25]. This is obvious from the fact that K contains the diagrams shown in Fig. 10a, while G contains the diagrams shown in Fig. 10b.

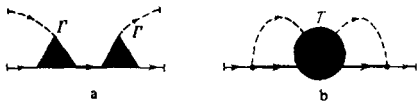

FIG. 10. Diagrams illustrating the agreement of the spectra of the single-particle (electron) and two-particle (electron + phonon) Green's function.

FIG. 11. Diagram illustrating the presence of electron-spectrum excitation energies in the phonon Green's function spectrum.

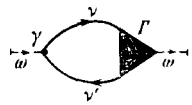

Since the number of phonons is not conserved, the poles of D and G are also interrelated. This relation can be easily established from the form of the phonon polarization operator $\mathscr{P}$ (Fig. 11). It differs from zero only if one G-function in the loop is retarded, as usual, and the other is advanced and therefore proportional to the number of electrons. Integrating in $\mathscr{P}$ with respect to the electron frequency, we can easily see that all the singularities in $\mathscr{P}$ are situated at the frequencies $\omega = \epsilon_{\nu\nu'} \equiv \epsilon_\nu - \epsilon_{\nu'}$, which are the excitation frequencies in the renormalized electron spectrum. As a result all the poles of D which are connected with the electron-phonon interaction have residues proportional to the electron concentration and located at the frequencies $\epsilon_{\nu\nu'}$. Therefore the electron-excitation spectrum can be determined equally well from the function D and interpreted as the perturbed phonon spectrum.

In conclusion we indicate a criterion that enables us to neglect the dispersion of the optical phonons, which can usually be expressed in the form

$$\omega_q = \omega_0 - \frac{q^2}{2\mu}, \quad (3.10)$$

where μ is of the order of the geometric mean of the electron and nuclear masses. The essential values of q are determined by the nonlocality radii of the kernels of Eqs. (3.7) and (3.8); they turn out to be of the order of the reciprocal of the dimension a of the electron state interacting with the phonons. The phonon dispersion can be disregarded if the phonon "kinetic energy" $\Delta\omega_q \sim 1/\mu a^2$ is much smaller than the energy scale of the spectral fine structure resulting from the electron-phonon interaction. Explicit estimates will be given in the analysis of particular systems. Analogous considerations apply also to the uncertainty, due to the finite lifetime of the phonon, in the phonon energy γ.

4. POLARON SPECTRUM

We start with the simplest system, the polaron, i.e., an electron interacting with polarization phonons.

a) Weak coupling—threshold singularity. It is obvious that here $E_1(p) = E_2(p) = p^2/2m$ and calculation of $\mathscr{M}^0$ in accord with (2.3) with allowance for (1.3) and (1.4b) yields[2)]

$$\mathscr{M}^0(\varepsilon p) = -\alpha\omega_0\frac{p_0}{p}\operatorname{arctg}\left[\frac{p^2}{2m(\omega_0-\varepsilon)}\right]^{1/2}. \quad (4.1)$$

At $p \approx p_0$ and $\epsilon \to \omega_0$ we obtain the relation (2.5) with

$$A = \alpha\omega_0\frac{\pi}{2}, \quad B = \alpha\omega_0^{1/2}. \quad (4.2)$$

Since $\mathscr{M}^0$ remains finite, the character of the spectrum is determined completely even in this order of perturbation theory. The spectrum has an end point, near which

weak pinning with tangency takes place (Fig. 2, curve 2)[19]. Since the total momentum of the system is conserved, states with definite values of the momentum should be marked on schemes of the type of Fig. 1; in view of this remark, it is easily understood that we are dealing here with the case of Fig. 1a.

To the contrary, as $\epsilon \to \omega_0$ states with p = 0 correspond to the case of Fig. 1c. Here $\mathcal{M}^0 \propto (\omega_0 - \epsilon)^{-1/2}$, and it is necessary to sum the entire chain of Fig. 4. This leads to

$$\mathcal{M} = -\alpha\omega_0\left(\sqrt{1-\frac{\varepsilon}{\omega_0}}-\alpha\right)^{-1}, \tag{4.3}$$

and the equation for the determination of the spectrum $\epsilon = \mathcal{M}(\epsilon)$ has a root $\epsilon = \epsilon_0$ that coincides exactly with the threshold. Therefore in this approximation, which corresponds to a binding-energy scale, $W \sim \alpha^2\omega_0$, there are no bound states, as indicated in[12].

This does not exclude in principle the possibility of formation of states with W having a higher order of smallness in α, but corresponds to allowance of diagrams of higher order in the irreducible four-point diagram in comparison with Fig. 4. This therefore calls for a more complete analysis, which was carried out by Matulis[13] using a generalized threshold technique for the calculation of $\mathcal{M}$ and Γ and the Ward identity. The result has shown that the general structure of $\mathcal{M}$ and Γ near the threshold remains the same as for the chain of Fig. 4 in a finite interval of values of α (in any case at $\alpha \lesssim 0.26$), and that there are no bound states in this entire interval.

The singularities in the interband absorption spectra, to which the variation of the spectrum near the end point $p \approx p_0$ should lead, were discussed in[26,27]. However, in these papers they ignored the Coulomb attraction of the electron and hole, which is of decisive significance; we shall therefore not discuss these singularities in greater detail.

b) Strong coupling—bound states. In the case of strong coupling, a polaron with $p \approx 0$ is an electron situated at a discrete level (with $E_0 \approx -0.32\alpha^2\omega_0$) in the field of the self-consistent polarization of the lattice; the effective mass of the polaron is $m^* \approx 2.3 \times 10^{-2}\alpha^4 \times m$[28-30a]. The binding energy of any complex including a phonon should, naturally, be lower than ω_0. Since the scale of the electron energies is $\alpha^2\omega_0 \gg \omega_0$, the bound states are more conveniently sought by using the phonon spectrum of a polaron-containing crystal (see the end of Chap. 3). At $\alpha \gg 1$, according to Pekar[31], the lattice vibrations can be described classically, and the state of the electron follows the ions adiabatically. Therefore the equation that determines the spectrum of the phonon frequencies in the crystal in the presence of a polaron is easiest to obtain semiclassically, by considering the polarization of the electron cloud in the lattice-polarization field. Since $m^* \propto \alpha^4$ is still large, the recoil of the polaron following emission of a phonon can be neglected; the bound states of the polaron and the phonon then acquire the meaning of local vibrations of the lattice near the polaron. The same equation is contained also in the quantum adiabatic theory of the polaron[30b].

As applied to a polaron at rest, the equation for the electric potential φ of the lattice polarization corresponding to oscillations with frequency ω is

$$(\omega_0^2-\omega^2)\Delta\varphi(\mathbf{r}) = -8\pi\alpha\omega_0^2 v_0 \int d^3\mathbf{r}' \sum_{n>0} \frac{\psi_0(\mathbf{r})\psi_n(\mathbf{r})\psi_0^*(\mathbf{r}')\psi_n^*(\mathbf{r}')}{E_n - E_0}\varphi(\mathbf{r}'), \tag{4.4}$$

where ψ_n and $E_n (n > 0)$ pertain to excited levels of the Hamiltonian $\mathcal{H}_0$ describing the electron in the polarization well corresponding to the ground state of the polaron (with electron function ψ_0). Equation (4.4) is inconvenient because the kernel includes all the ψ_n. The situation changes, however, if we go over from (4.4) to the corresponding extremal principle and introduce in place of φ a new function f in accordance with

$$\psi_0\varphi = (\mathcal{H}_0 - E_0)\psi_0 f. \tag{4.5}$$

This is possible, inasmuch as the quantity φ determined from (4.4) contains an arbitrary additive constant. We ultimately obtain for the determination of φ the following equation[12]

$$\frac{\omega_0^2-\omega^2}{16\pi\omega_0^2} = \max_f\left\{\frac{\int d^3\mathbf{r}\psi_0^2(\nabla f)^2}{\int d^3\mathbf{r}\left[\nabla(\Delta f + 2\nabla f\nabla\ln\psi_0)\right]^2}\right\}. \tag{4.6}$$

All the lengths on the right-hand side of (4.6) are expressed in units of $(2m\alpha^2\omega_0)^{-1/2}$, and since all the parameters have been left out the relative binding energies $W/\omega_0 = (\omega_0 - \omega)/\omega_0$ are universal.

It is interesting that in (4.6) the entire information concerning the electronic spectrum of the polaron reduces to a single function ψ_0, which can be obtained with high accuracy. Since ψ_0 is spherically symmetrical and the right-hand side of (4.6) is positive-definite, there exist extremals of f with all value of the angular momentum; consequently, there exists an infinite number of eigenvalues $\omega_r < \omega_0$. For the lower levels, an estimate yields $W_r = \omega_0 - \omega_r \approx (0.10-0.15)\omega_0$.

Inasmuch as all these states lie under the threshold and W_r is much smaller than ω_0 (to be sure, the smallness is here numerical and not literal), they can be naturally interpreted as bound states of a polaron and a phonon. If account is taken of the dependence of their energy on the total momentum p of the system then we arrive at the conclusion that, at least near p = 0, new branches of the spectrum are produced and constitute lower excited states of the polaron. Since $|E_0| \gg \omega_0$, multiple frequencies $s\omega_r$ should be observed in the spectrum; at $s > 1$, however, they are damped.

The experimental consequences of the existence of a bound-state spectrum have not yet been investigated. Therefore, although the bound states should apparently greatly influence a number of kinetic phenomena, all that can be stated at present with assurance is that a system of satellites is produced near the fundamental lattice-absorption and Raman-scattering bands.

Comparing the results on weak and strong coupling, we arrive at the conclusion that the first bound state should occur at a certain α_c, the value of which, however remains unknown so far. In the crystals experimentally investigated to date, $\alpha \lesssim 3$. It is therefore of great interest whether α_c falls in this region. The available preliminary estimates give grounds for hoping that this is the case and $\alpha_c \approx 1$ (or even <1; cf.[13]).

5. IMPURITY CENTERS

We consider now the problem of the impurity center, i.e., an electron situated on a local level in the field of the defect and interacting with the phonons. Owing to the electron-phonon interaction near the center, the

spectrum of the phonons is perturbed and this can give rise to localized electron plus phonon bound states, which in another language can be described as a special type of local phonon modes. Their appearance has nothing in common with the usual mechanism of local-mode formation (which are connected with the mass differences and also with the changes in the rigidities of the couplings as a result of changes in the configurations of valence electrons) and is due entirely to the interaction between the weakly-bound impurity electron and the phonons. They are called dielectric modes. Depending on the relation between ω_0 and the ionization potential R of the center, the situation can be either resonant or nonresonant. In weak coupling, this problem can be analyzed in general form[24], so that it is possible to trace the transition between different limiting cases. The experimental data obtained by now confirm convincingly the existence of dielectric modes.

a) Hybrid and bound states. We assume henceforth only that the ground state of the center is not degenerate, and in all other respects the model of the center is arbitrary.

Calculation of $\mathcal{M}^0$ in accordance with (2.3) leads to (2.5d), i.e., it is necessary to sum the series of Fig. 4. The situation is much more complicated than with the polaron and the magnetopolaron (cf. Chaps. 4 and 7), because $\mathcal{M}$ and Γ are not diagonal in the quantum numbers of the electronic levels. However, because of the unique circumstance that the spectrum of the electron subsystem is discrete, the standard equation (3.7) for Γ can be reduced to an equation that determines $\mathcal{M}$ directly.

This equation is

$$\mathcal{M}^{-1}(\varepsilon) = (\varepsilon - \omega_0 - E_0) A^{-1} - G^0(\varepsilon - 2\omega_0), \tag{5.1}$$

where

$$A_{ss'} = \int \frac{d^3\mathbf{q}}{(2\pi)^3} \gamma_{s0}(\mathbf{q}) \gamma_{0s'}(-\mathbf{q}). \tag{5.2}$$

The subscripts s and s′ in the vertices $\gamma_{ss'}(q)$ number all the electronic levels of the center; s = 0 corresponds to the ground level.

It can be shown that the usual equation for the poles of G

$$\mathrm{Det}\ \|\mathcal{M}^{-1} - G^0\| = 0 \tag{5.3}$$

together with (5.1) leads to the equation[24]

$$\mathrm{Det}\left\| A_{ss'} - \delta_{ss'} W(E_s - \omega_0 + W) \frac{\omega_0 + E_s}{2E_s} \right\| = 0 \quad (s, s' = 1, 2, \ldots, \infty). \tag{5.4}$$

In (5.4), E_S is the excitation energy of the center (henceforth $E_0 = 0$), and $W = \omega_0 - \epsilon$ is the binding energy of the complex, which will be referred to here as the binding energy of the phonon. We emphasize that we have excluded here the values s, s′ = 0.

Using the general equation (5.4), it is convenient to consider limiting cases. If the system is close to resonance, $E_S \approx \omega_0$ (Fig. 1a), or more accurately if

$$|E_s - \omega_0| \ll \Delta E, \tag{5.5}$$

where ΔE is the characteristic distance between the electron levels, then it suffices to use a two-level scheme, i.e., to take into account only one excited level. Then (5.4) reduces to

$$A_{ss} = W(E_s - \omega_0 + W), \tag{5.6}$$

which coincides with the equation obtained by Kogan and Sirus in[10], in which dielectric modes were predicted. Equation (5.6) is equivalent to the single-phonon approximation, as is in general typical of the resonant situation. For the PO interaction we have $A_{ss} \sim \alpha\omega_0(R\omega_0)^{1/2}$.

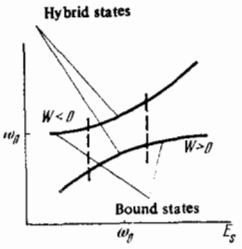

FIG. 12. Hybrid and bound state for an impurity center in a two-level scheme (it is assumed that $E_0 = 0$).

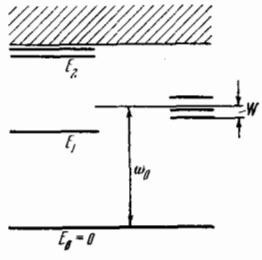

FIG. 13. Level scheme of impurity center under nonresonant conditions. Left–electronic levels, right–levels of the bound states of the phonon with the center (frequencies of local modes). The figures shows the case when one electron frequency $E_1 < \omega_0$.

In the immediate vicinity of the resonance we have

$$W \approx A_{ss}^{1/2}, \quad \text{если } |E_s - \omega_0| \ll A_{ss}^{1/2}. \tag{5.7a}$$

At a certain distance from resonance we have

$$W \approx A_{ss}/(E_s - \omega_0), \quad \text{если } A_{ss}^{1/2} \ll |E_s - \omega_0|. \tag{5.7b}$$

At resonance we have $\langle N \rangle \approx 1/2$ for both modes, i.e., hybrid states are produced. With increasing distance from resonance (on going from (5.7a) to (5.7b)), we have $N \to 1$ for the level (5.7b) remaining near ω_0; a bound state is therefore produced. The second root $\omega \approx E_S$ corresponds to a state with $\langle N \rangle \sim \alpha$. The course of the levels near resonance is shown schematically in Fig. 12. We emphasize that we have here bound states with both W > 0 and W < 0, this being a consequence of the discrete character of the electronic spectrum in the absence of dispersion of the phonon frequencies.

Outside the narrow interval (5.7a), Eq. (5.4) takes on the simpler form

$$\mathrm{Det}\left\| A_{ss'} - \delta_{ss'} W \frac{E_s^2 - \omega_0^2}{2E_s} \right\| = 0 \quad (s, s' = 1, 2, \ldots, \infty); \tag{5.8}$$

it describes the situation of Fig. 1c. The quantity W enters in this equation linearly and therefore (5.8) can be easily investigated by the usual algebraic methods. If all $E_S > \omega_0$, then all W > 0. If there are several $E_S < \omega_0$, then we get as many roots W < 0. For centrally-symmetrical centers there exists states corresponding to all values of the angular momentum. It is very important that each value of the angular momentum corresponds to an infinite number of different W.[3)]. The level scheme is shown in Fig. 13.

Equation (5.8), while convenient for a qualitative assessment, is inconvenient for a quantitative determination of W. We can return however, to the configuration representation[24,34]; then (5.8) is transformed into

$$2A(\mathscr{H}_0 - E_0)\psi = W[(\mathscr{H}_0 - E_0)^2 - \omega_0^2]\psi, \tag{5.9}$$

where $\mathscr{H}_0$ is the Hamiltonian of the electron at the

center without the interaction with the phonons, and the integral operator is

$$A(\mathbf{r}, \mathbf{r}') = \psi_0(\mathbf{r}) V(\mathbf{r}-\mathbf{r}') \psi_0(\mathbf{r}'), \quad V(\mathbf{r}) = \int \frac{d^3\mathbf{q}}{(2\pi)^3} |c_q|^2 e^{i\mathbf{q}\mathbf{r}}. \tag{5.10}$$

For interaction with polarization phonons we have

$$V(\mathbf{r}) = \frac{e^2\omega_0}{2r\bar{\varkappa}}. \tag{5.11}$$

An estimate of the binding energy yields for this case

$$W_\Gamma = b_\Gamma \omega_0 [(\varkappa_0/\varkappa_\infty) - 1] = b_\Gamma \alpha \omega_0 (\omega_0/R)^{1/2}. \tag{5.12}$$

The factors b_Γ can be determined from (5.9) by a variational method; $b_\Gamma \approx 0.1$ for the lower levels. It is of interest that at fixed $\varkappa_0/\varkappa_\infty$ the binding energy is independent of R.

b) Experimental investigation of dielectric modes. It appears that the influence of resonant interaction with phonons on the impurity-electron spectrum was first investigated for Bi donors in Si. Onton et al.[5] have proposed that the anonomously large width of one of the bands in the donor spectrum is due to resonant interaction with TO⟨100⟩ phonons, and have shown experimentally that uniaxial deformation causes the band to split in two, with one of the components becoming narrow rapidly. These results can be easily understood if it is recognized that, owing to the finite dispersion of the phonons, the dielectric mode is produced only at a definite ratio of ω_0 to the excitation energy of the spectrum. Analogous data are available for Ga in Si[35] and Te in AlSb[36].

Dielectric modes were observed under nonresonant conditions by Dean et al.[37] for the donors S, Te, Si, and Sn in GaP. The excitation energy ranges from 58 to 94 meV at $\omega_0 = 50$ meV; the following binding energy is $W \sim 1$ meV. It was of particular interest that modes with different symmetries were separated. It was shown theoretically in[37a] that p-modes should predominate in Raman scattering, and these modes were obtained experimentally for all impurities. At the same time, s-modes were found in the phonon satellites of the emission bands of impurity excitons; additional weak satellites were ascribed to d-modes.

An even richer spectrum of bound states of phonons was observed in the emission spectrum of impurity excitons in CdS[38], and is shown in Fig. 14. For the acceptors to which the excitons are bound we have $R \approx 4\omega_0$, i.e., the system is very far from resonance. Although the authors of[38] have classified the observed modes as being of the s, p, and d type, the parity selection rules predict predominance of modes with even angular momenta; it is possible that only s-type modes are present in the spectrum of Fig. 14. It is important to note that owing to the negative dispersion of the phonons the levels of the bound states are superimposed on the spectrum of the short-wave phonons; consequently the bound states are metastable. It is therefore of special interest that although the density of the phonon spectrum in the region of the bound states is large (this pertains in particular to the lower level), nevertheless the bands corresponding to bound states are narrow and are distinctly seen.

The luminescence spectrum of impurity excitons bound to neutral donors was recently observed also in CdS and CdSe[39]. For donors we have $R < \omega_0$, so that strictly speaking no bound states exist. Nonetheless, a

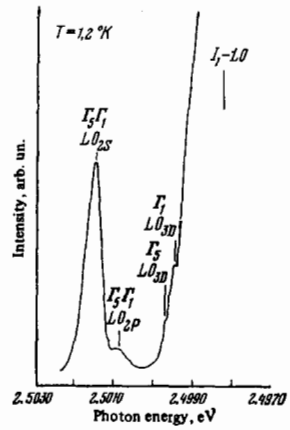

FIG. 14. Phonon satellites in the luminescent spectra of impurity excitons in CdS (from [38]). The high intensity band on the right corresponds to the lattice phonons, and the remaining bands to bound states of the phonon.

distinct structure has been observed in the spectra, and seems to indicate that the resultant states have considerable lifetimes.

Thus, dielectric modes have already been observed in the resonant[5], intermediate[37], and nonresonant[37,38] situations. Their main properties agree well with theory. In[37a,38], they obtained also satisfactory quantitative agreement between the theoretical and experimental values of W; this agreement, however, should not be regarded as too significant, since it seems to be the result of the fact that the errors connected with the use of the two-level approximation and the simplified model of the center cancel each other to a considerable degree.

6. EXCITON-PHONON COMPLEXES

The next system in order of complexity is the exciton, in which, in comparison with the impurity center, a new parameter appears, namely the mass of the hole. The physical difference is connected mainly in the fact that owing to the finite mass the exciton experiences recoil when it emits a phonon, as a result of which the divergence (2.5d) gives way to the much weaker singularities (2.5a) and (2.5b).

The interest in the exciton-phonon complexes was aroused by the experimental data of Liang and Yoffe[4]. They observed in the exciton-absorption spectrum of ZnO, where the situation corresponds to Fig. 1b, an absorption maximum near the phonon emission threshold, and ascribed it to a "complex." The spectra of a number of other crystals were subsequently investigated from analogous points of view.

We consider below the main theoretical premises concerning the conditions for the formation of exciton-phonon complexes and discuss the experimental data briefly from this point of view. Unfortunately, the interpretation of the data on exciton-phonon complexes is still highly preliminary.

a) Discrete spectrum in the resonance situation. We consider first the resonance situation (Fig. 1a) and confine ourselves to the results that can be obtained in accordance with standard perturbation theory in the single-phonon approximation. Separating the motion of the center of gravity of the electron and confining ourselves to states with total momentum $\mathbf{P} = 0$, we obtain for the interaction with the polarization phonons, in place of (2.3),

$$\mathcal{M}^0_{ss'}(\varepsilon) = \int \frac{d^3\mathbf{q}}{(2\pi)^3} \mathcal{B}(q) \sum_{\bar{s}} \frac{\langle s|\rho_{\mathbf{q}}|\bar{s}\rangle\langle\bar{s}|\rho^+_{\mathbf{q}}|s'\rangle}{\varepsilon - E_{\bar{s}} - \omega_0 - (q^2/2M) + i0}, \tag{6.1}$$

where

$$\rho_q(\mathbf{r}) = \exp\left(i\frac{m_2}{M}\mathbf{qr}\right) - \exp\left(-i\frac{m_1}{M}\mathbf{qr}\right),\ M = m_1 + m_2; \qquad (6.2)$$

m_1 and m_2 are the masses of the electron and hole; the subscript s labels the Coulomb levels. The presence of the term $q^2/2M$ in the denominator eliminates the divergence. We can therefore confine ourselves to the single-phonon approximation. The threshold behavior of $\mathcal{M}^0$ is determined by the behavior of $\langle s|\rho_q|s'\rangle$ as $q \to 0$. This gives rise to two possibilities, depending on whether the matrix element $\langle s|r|s'\rangle$ is different from zero for the pair of states s and s′ for which $|E_s - E_{s'}| \approx \omega_0$.

If it differs from zero (for example, a pair of states of the s and p type), then we obtain (2.5b) with

$$A \sim \alpha_m \frac{M}{m}\omega_0,\ B \sim \alpha_m\left(\frac{M}{m}\right)^{3/2}\omega_0^{1/2}; \qquad (6.3)$$

here α_m was calculated in accordance with (1.5) for the reduced mass m. Therefore, according to Chap. 3, exciton-phonon complexes and pinning arise in this case; the picture is graphically described by curve 2 of Fig. 2[18]. At the threshold we have $Z \to 0$ in accordance with (1.5), and the probability of exciton absorption vanishes.

If $\langle s|r|s'\rangle = 0$ (for example, both states are of the s-type), then we arrive at (2.5a) with

$$A \sim \alpha_m \frac{M}{m}\omega_0,\ B \sim \alpha_m\left(\frac{M}{m}\right)^2,\ C \sim \alpha_m\left(\frac{M}{m}\right)^{5/2}\omega_0^{-1/2}. \qquad (6.4)$$

Consequently, no complexes are produced if α_0 is small enough, there is no pinning (curve 1 of Fig. 2), and the absorption probability varies slightly near the threshold[18]. Beyond the threshold, weak damping proportional to $(\epsilon - \omega_0 - E_S)^{3/2}$ is produced, and the state s′ can be regarded as quasistationary.

It is very important that the factor M/m is contained in (6.4) in all the increasing powers. If $M/m \gg 1$, then it is possible to have $B \sim 1$ even in the region where the usual weak-coupling criteria are satisfied for both particles ($\alpha_m \ll 1$, $\alpha_M = \alpha_m(M/m)^{1/2} \ll 1$), The contribution of the phononless states at the threshold $Z \approx (1 + B)^{-1}$ is then noticeably smaller than unity, i.e., complexes are produced. Consequently, the weak-coupling criterion is violated early at $M/m \gg 1$, and the theory should be generalized. This was done by a variational method by Toyozawa and Hermanson[11,40], who constructed for the 2s state a single-phonon approximation variant in which account was taken of the ground-state virtual phonons; the greatest changes appear in the dependence of the intensity of the exciton absorption on $E_{S'} - E_S$, which becomes nonmonotonic. A generalization to the case of the p-states is given in[41].

In the limit as $M/m \to \infty$ the properties of the exciton become identical with the properties of the impurity center, and in this case (Chap. 5) a system of bound states arises also off resonance (the situation of Fig. 1c). It is therefore natural to assume that at $M/m \gg 1$ they should occur also for excitons. Although there is still no systematic theory, an estimate based on allowance for the recoil leads to the following criterion for the formation of nonresonant bound states[24]:

$$\frac{m}{M} \leqslant 0.1\frac{\kappa_0}{\bar{\kappa}}\frac{\omega_0}{R}, \qquad (6.5)$$

which is stringent, but not excessively so.

In the crystals BeO[42], MgO[42,43] and AgBr[44-46] there were observed, in addition to the ground exciton band, transitions to the excited state, which is located above the ground state at a distance $\Delta\omega$ such that $\Delta\omega < \omega_0 < R$. The hypothesis was advanced that this excited state is an exciton-phonon complex and explains, for example, the anomalously high intensity of the transition to the excited state in MgO. However, since no special experiments in which the distance between electronic levels could be varied were performed, there is no proof that this assumption is valid.

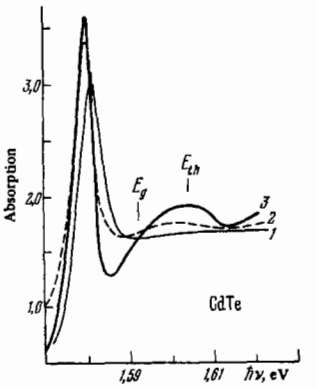

FIG. 15. Exciton-absorption spectrum of CdTe at 77° K in accordance with [50] (2) and theoretical spectrum (after [47]) (3). For comparison, curve 1 corresponds to the absence of exciton-phonon interaction. The markers E_g and E_{th} show the end point of the electron-hole continuum and the phonon-emission threshold.

b) Absorption in the ionization continuum near threshold. We proceed to the situation in Fig. 1b. The exciton-phonon absorption falls in this case in the region of the electron-hole continuum. Therefore a consistent allowance for the electron-phonon interaction should lead to a more complicated picture than for the indirect transitions in Ge and Si, where the situation reduces to the appearance of the known "steps." In this case, a comparable contribution is made by the change in the probability of the purely electronic transitions that lie in the same region of the spectrum.

The standard perturbation-theory series for the exciton Green's function F leads in second order to the following formula for the conductivity[47]

$$\sigma(\omega) \sim \mathrm{Im}\sum_{ss'}\psi_s(0)\psi_{s'}^*(0)\left\{F_s^0(\omega)\delta_{ss'} + F_s^0(\omega)\int\frac{d^3\mathbf{q}}{(2\pi)^3}\mathscr{F}(q)\langle s|\rho_q|0\rangle F_0^0(\omega - \omega_0 - (q^2/2m))\langle 0|\rho_q^+|s'\rangle F_{s'}^0(\omega)\right\}. \qquad (6.6)$$

In the second term, the residues connected with F_0^0 describe absorption with production of a 1s-exciton and a phonon, while the residues connected with F_S^0 and $F_{S'}^0$ describe the change of the absorption in the electron-hole continuum; $\psi_S(\mathbf{r})$ are the Coulomb wave functions.

Figure 15 shows the results of the tabulation of (6.6) as applied to the parameters of CdTe, with a phenomenological width introduced for the exciton levels. We see that the exciton ground band is followed by a satellite, the maximum of which is located near the phonon emission threshold E_{th}.

It is precisely a structure of this type, observed in ZnO[4] and then in other crystals (TlBr, TlCl[48,49], CdS, CdSe, CdTe[50]) which served as the stimulus for the discussion of the problem of "complexes." However, as follows from the foregoing, it can be explained within the framework of simple perturbation theory; it is seen from Fig. 15 that the agreement between the experimental and theoretical data for CdTe is satisfactory. Yet in (6.6) the maximum is a result of a pure interference effect (of the type of the Fano effect[51]). It must be specially emphasized that formula (6.6), having

been obtained in a finite order of perturbation theory for F, cannot contain in principle any bound and quasibound states. Of course, one cannot exclude the possibility of some complicated formations occurring in crystals with a large electron-phonon coupling (such as TlCl and TlBr) near the threshold. However, the attempt made so far[52] to formulate the "complex" concept theoretically in terms of quasibound states of the exciton and the phonon was not successful, because the imaginary part of the mass operator (damping) turned out to be larger than the real part.

7. MAGNETOPOLARON

The question of the calculation of the spectrum of the magnetopolaron near the decay threshold arose in connection with experiments on interband magnetoabsorption and cyclotron resonance, which have exhibited an unusual behavior when the cyclotron frequency ω_c coincided with the frequency of the longitudinal optical phonon $\omega_0 \equiv \omega_{LO}$ (see Sec. (d) of this chapter and Chap. 8[4]). The theory for this resonant case was constructed in essence on the basis of the single-phonon model[8,9]. Near the threshold, a structure is produced in the spectrum with a characteristic scale $\alpha^{2/3}\omega_0$, and is responsible for the singularities in the absorption. However, since the behavior of the mass operator in the single-phonon model near the threshold $\epsilon = \omega_0$ is determined by an expansion of the type (2.5c), it turns out that in spite of the weakness of the coupling ($\alpha \ll 1$) there exists near the threshold a region where perturbation theory (expansion of $\mathcal{M}$ with respect to α) does not hold for the mass operator. This circumstance is not connected in any way with the resonance $\omega_c = \omega_0$. A calculation of the next higher terms of the expansion of $\mathcal{M}$ shows that $\mathcal{M}^0$ predominates at $|\epsilon - \omega_0| \gg \alpha\omega_0$. This estimate justifies the calculation of the resonant structure of the spectrum with scale $\alpha^{2/3}\omega_0$; however, this raises simultaneously the question whether there exists a finer structure of the spectrum in that region of the threshold where perturbation theory does not hold.

The diagrams for $\mathcal{M}$ without intersection of phonon lines become significant at $|\epsilon - \omega_0| \sim \alpha\omega_0$. They can be easily summed in all orders in α[14,54]; this leads to an expression for which differs from M^0 only in a renormalization of the fraction of the threshold, by an amount on the order of $\alpha\omega_0$. In the region $|\epsilon - \omega_0| \lesssim \alpha^2\omega_0$, however, diagrams with intersections become important. Their summation is possible only by the method described in Chap. 3. When this procedure was first carried out[16] it turned out that in the near-threshold spectrum there exist in a region on the order of $\alpha^2\omega_0$ additional branches of the spectrum, describing bound states of the electron and phonon.

a) Fundamental equations. To set up the equations of Fig. 3 as applied to the magnetopolaron it is necessary first to separate the set of quantum numbers corresponding to the dangerous cross sections. This set comprises the Landau quantum number n, the longitudinal (along H) component of the electron momentum $k_z \equiv k$, one of the transverse components of the electron momentum (say k_x), and the two phonon-momentum components $q_\perp$ and $q_\parallel$. The equations become much simpler because the exact Green's function G is diagonal in n, k, and k_x and does not depend on k_x. We note that the diagonality of G with respect to n[55,56] is far from trivial—the symmetry group responsible for it is still unknown at present. The total energy in the dangerous section $n\omega_c + (1/2m)k^2 + \omega_0$ depends only on n and k, and consequently the set ν, on which G^0 depends critically near the threshold (see Chap. 3), must consist of these two quantum numbers. Then $\nu = 0$ corresponds to $n = 0$ and $k = 0$; in the summation over n it is therefore necessary to retain only the term $n = 0$, and the main contribution to the integral with respect to k is made by states with $k = 0$. The quantum number $q_\parallel$ can be eliminated as a result of the existence of the integral of motion $p = k + q_\parallel$, which is the total longitudinal momentum of the electron + phonon pair. It is possible to eliminate k_x analogously, since $q_x + k_x$ is also an integral of the motion. As a result, only integration with respect to two quantum numbers $q_\perp$ remains in the dangerous cross section, and it is these numbers which play the role of the quantities Q in Chap. 3. Consequently, it is precisely with respect to $q_\perp$ that the integration is carried out in equations of the type (3.7) and (3.8).

It should be noted that the spectrum of the electrons plus phonon pair does not depend on $k_x + q_x$, just as the spectrum of the electron does not depend on k_x. It is most convenient to eliminate immediately the quantum numbers k_x by changing over to the gauge-invariant technique[56].

An equation of the type (3.7) for the vertex Γ was first obtained and solved for the case $\omega_c \gg \omega_0$ in[16]; a more general investigation was carried out in[22]. We shall henceforth use a more convenient equation of the type (3.8) for the scattering amplitude T[25]. Using the gauge-invariant technique, one can choose such a definition of the four-point diagrams T and $\square$ that these quantities turn out to depend on the difference $\varphi - \varphi'$ between the azimuthal angles of the vectors $q_\perp$ and $q'_\perp$. Therefore, if we expand these quantities in a Fourier series of the type

$$T(q_\perp, q'_\perp) = \sum_{l=-\infty}^{\infty} e^{il(\varphi-\varphi')} T_l(t, t'), \tag{7.1}$$

where

$$t = \frac{1}{2}a^2q_\perp^2, \quad a = \left(\frac{c}{eH}\right)^{1/2}, \tag{7.2}$$

then we can use explicitly the axial symmetry of the problem and determine the angle variables in the integral equation. The equation for T is then transformed into a series of equations for $T_l (-\infty < l < +\infty)$. The kernels of these equations are the Fourier components $\square_l$ of the kernel $\square$. In place of Λ it is more convenient to use the mass operator, which is proportional to it,

$$\mathcal{M}^0(\varepsilon) = -i\tilde{\alpha}\omega_0 \frac{p_0}{\sqrt{2m(\varepsilon-\omega_0)+i0}}, \quad \operatorname{Im}\mathcal{M}^0(\varepsilon) < 0, \tag{7.3}$$

where

$$\tilde{\alpha} = \frac{1}{2}\alpha\frac{\omega_c}{\omega_0}, \quad p_0 = \sqrt{2m\omega_0}. \tag{7.4}$$

If we change over to the dimensionless quantities

$$\lambda = -\frac{1}{\omega_0}\mathcal{M}^0, \quad L_l = -\omega_0\square_l, \quad R_l = -\omega_0 T_l,$$

then the equations for T_l assume the standard form of the Fredholm equations for the resolvent:

$$R_l(\varepsilon p; t, t') = L_l(p; t, t') + \lambda(\varepsilon)\int_0^\infty d\bar{t} L_l(p; t, \bar{t}) R_l(\varepsilon p; \bar{t}, t'). \tag{7.5}$$

It is now clear that T has a singularity in ϵ when

$\lambda(\epsilon)$ coincides with one of the eigenvalues $\lambda_l^r(p)$, $r = 1, 2, \ldots$ of the kernel. The singularity corresponds to the bound state if it lies below the threshold, i.e., at $\epsilon < \omega_0$, when $\lambda(\epsilon) > 0$. Thus, the spectrum of the bound states is determined by the positive part of the spectrum of the integral equation, and from (7.3) follows the dispersion law

$$\varepsilon_l^r(p) = \omega_0 \left\{1 - \frac{\tilde{\alpha}^2}{[\lambda_l^r(p)]^2}\right\}, \qquad \lambda_l^r(p) > 0, \quad l = -\infty, \ldots, +\infty, \quad r = 1, 2, \ldots \tag{7.6}$$

The extent to which such an approach is constructed is determined by the real possibilities of investigating the spectrum of the kernel. Let us write it out, for example, for the most interesting case $p = 0$;

$$L_l(t, t') = [\Phi(t)\Phi(t')]^{1/2} e^{-(t+t')/2} \sum_{s=0}^{\infty} \frac{1}{s!}(tt')^{s/2}\left[J_{l+s}(2\sqrt{tt'})\frac{\sigma}{s+\sigma} + \delta_{l,s}\frac{\sigma}{s-\sigma}\right], \tag{7.7}$$

where J_l is a Bessel function and

$$\Phi(t) = \begin{cases} 1, & \text{DO}, \\ \dfrac{\sigma}{t}, & \text{PO}, \quad \sigma = \dfrac{\omega_0}{\omega_c}. \end{cases} \tag{7.8}$$

Such a kernel can be investigated only in various limiting cases; this suffices, however, to obtain a qualitative picture of the spectrum and to establish the principal irregularities. These will be given in the next section, and we shall indicate here briefly the methods of investigating the nucleus.

In strong fields ($\sigma \ll 1$), only the term with $s = 1$ remains in the sum (7.7). For a DO interaction we can obtain at $l \neq 0$ the exact solution[25] by using the invariance of Laguerre polynomials with respect to the Bessel transformation. At $l = 0$, this is hindered by the second term in the bracket of (7.7); since this term, however, yields a factorizable part of the kernel, the problem for the spectrum of the kernel can be reduced to a transcendental equation. As a result it turns out that for any l there exists an infinite sequence of positive eigenvalues, increasing without limit, which means in accordance with (7.6) the existence of a series of bound states that condense towards the threshold. For the more important PO interaction it is impossible to obtain an exact solution. However, by comparing the behavior of the kernel at $t = 0$ and $t = \infty$ for PO and DO, and using some general theorems of the theory of integral equations, it can be shown[25] that the spectrum for PO is qualitatively the same as for DO.

In weak fields ($\sigma \gg 1$) the Bessel-function series can be re-expanded in a series of the type $\sum_s \sigma^{-s}(tt')^{s/2}$, and the kernel can be approximated by degenerate kernels[22]. In this case, too, the spectrum contains an infinite number of positive eigenvalues that increase without limit, so that the series of the bound states exists also in weak fields.

An integral equation of the type (3.7) for the vertex Γ can be investigated in similar fashion, and this can yield the spectrum of the single-particle electronic Green's function G. It can be shown[25] that the spectrum $G_n(k)$ contains the spectra $T_l(p)$ with $-\infty < l < n$ and $p = k$. Therefore the spectrum of the aggregate $G_n(n = 0, 1, 2, \ldots)$ coincides with the spectrum of the aggregate $T_l(l = 0, \pm 1, \pm 2, \ldots)$, in full agreement with the general remark made in Chap. 3.

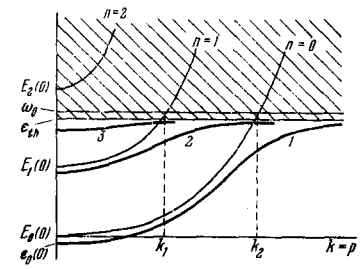

FIG. 16. Spectrum of magnetopolaron (the energy is reckoned from $E_0(0) = 0$).

b) Structure of the energy spectrum. When describing the magnetopolaron spectrum, it is necessary to distinguish between two situations: resonant, when $\omega_0 \approx \omega_c, 2\omega_c, \ldots$ (Fig. 1a), and nonresonant, when these frequencies are different, or where they can be of the same order of magnitude (Fig. 1c).

We consider first the second case, for which the spectrum is shown in Fig. 16. The thin lines represent the nonrenormalized Landau spectrum $E_n(k)$ of the electron, and the thick lines the true (renormalized) spectrum. If the bottom of the nonrenormalized band n lies below the threshold ω_0 (n = 0, 1 in the figure), then there exists such a branch of the true spectrum $\epsilon_l(p)$ with $l = n$, which differs little at momenta $p < k_n$ from the nonrenormalized branch. The threshold momentum k_n is determined from the condition $E_n(k) = \omega_0$. At $p \ll k_n$, the true spectrum differs from the nonrenormalized one only in a shift of the bottom of the band and in a change of the effective mass. Both effects are proportional to α. Obviously, the lowering of the bottom of the band n = 0 leads to a renormalization of the threshold—the true threshold $\epsilon_{th} = \epsilon_0(0) + \omega_0$ lies below nonrenormalized one ω_0. When p approaches k_n and ϵ approaches ϵ_{th}, a radical restructuring of the nonrenormalized branch takes place. At $p \approx k_n$, the spectrum does not reach the threshold and remains lower by an amount proportional to $\alpha^{2/3}\omega_0$. At $p > k_n$, the spectrum approaches the threshold asymptotically and remains below it at a distance proportional to α^2. This picture corresponds to the unlimited pinning described in Chap. 2.

In addition to these branches, which are genetically connected with the branches of the nonrenormalized spectrum (1 and 2 in Fig. 16), the true spectrum contains additional branches, the existence of which is due entirely to the interaction (3 in Fig. 16). The number of these branches is infinite, and all lie under the threshold at a distance proportional to α^2 and form a sequence that condenses to the threshold (not shown in the figure). The branches of the second type exist for quantum numbers l of both signs.

The states on the branches of the described two types differ significantly with respect to the average number $\langle N \rangle$ of the phonons that participate in their formation. On the branches of the first type $\langle N \rangle$ increases with increasing p, from $\langle N \rangle \sim \alpha$ at $p < k_n$ to $\langle N \rangle \approx 1$ at $p > k_n$ through $\langle N \rangle \approx \frac{1}{2}$ at $p = k_n$. The states on these modes are therefore bound electron-phonon states for all p. If we write the dispersion law of these modes in the form

$$\varepsilon(p) = \varepsilon_0(0) + \omega_0 - W(p), \tag{7.9}$$

where $\epsilon_0(0)$ is the renormalized bottom of the band

n = 0, then W is the binding energy. This interpretation is also favored by the following: Since the energy $\epsilon(p)$ of the elementary excitation is practically independent of its momentum p, it is clear that the contribution of the electron to the total momentum and the total excitation energy is small, for otherwise the dependence of ϵ on p would be just as large as in the nonrenormalized spectrum. Thus, the electron is at the bottom of the band n = 0, and the energy and momentum are carried almost entirely by the phonon; the electron determines only the charge and the spin of the elementary excitation.

We consider now the distinguishing features of the resonant situation, which arises starting with $\omega_c \approx \omega_0$ for modes with $l = 1$. If $\omega_c < \omega_0$, then the bottom of the band n = 1 lies lower than the threshold, and there exists a spectral mode with $l = 1$ and genetically connected with the nonrenormalized n = 1 band. On the other hand, if $\omega_c > \omega_0$, then there is no such spectral mode with $l = 1$. We consider therefore in greater detail the lower state with $l = 1$ and p = 0. An investigation shows that at $\omega_c < \omega_0$ this is a polaron state, i.e., $\langle N \rangle \sim \alpha$, and at $\omega_c > \omega_0$ it is a bound state, i.e., $\langle N \rangle \approx 1$. At the instant of passage through resonance $\omega_c = \omega_0$, the state in question becomes hybrid, i.e., $\langle N \rangle \approx 1/2$. It is important that in this case it lies below the threshold, at a distance on the order of $\alpha^{2/3}\omega_0$, i.e., much farther than the bound states. States with p = 0 at higher modes of the series $l = 1$ experience no qualitative changes whatever on going through the resonance, and are bound states for all H.

It is seen from this analysis that the transition from the polaron states to the bound states via hybrid states is possible both when p is varied and H is fixed, and vice versa. It is also obvious that for the series $l = 2, 3, \ldots$, the singularities will arise in weaker magnetic fields $\omega_c = \omega_0/2, \omega_0/3, \ldots$

The bound states considered above are due to the usual electron-phonon interaction (1.1), which is linear in the phonon amplitudes. In some cases an important role may be assumed by an interaction that is quadratic in these amplitudes; such an interaction can lead to electron-phonon binding in a magnetic field[57]. The binding energy turns out to be proportional to $|\langle \mathscr{H}_{eL} \rangle|^2$, and not to $|\langle \mathscr{H}_{eL} \rangle|^4$ as in the case of the linear interaction. For this reason, the binding energies may turn out to be of the same order of magnitude. The bound states produced in the quadratic interaction have a number of distinguishing features. In particular, they cannot be obtained as poles of G, and only as poles of T. This means that the electron is bound, as it were, not with the phonon that it emits itself, but with a phonon already present in the crystal. Allowance for the quadratic interaction leads also to the appearance of pinning at multiple and combination frequencies $2\omega_{LO}$, $2\omega_{TO}$, $\omega_{LO} \pm \omega_{TO}$, where ω_{LO} and ω_{TO} are the limiting frequencies of the longitudinal and transverse optical phonons. There are indications that a pinning of this type has been observed experimentally[58]. It is important to note in this connection that the quadratic interaction with TO phonons has a polarization character[57], although the linear interaction does not have this character.

c) Optical effects. The existence of electron plus phonon complexes influences strongly the spectral dependence of the optical effects in which the electron transition is accompanied by production of an optical phonon. Two groups of effects should exist in this case, one with a characteristic energy scale $\alpha^{2/3}\omega_0$ and due to the existence of hybrid states with p = 0 under magnetophonon-resonance conditions, and the other with a characteristic scale $\alpha^2\omega_0$ and due to the existence of bound states with p = 0.

The first group of effects can be investigated with the single-phonon model. Let us dwell in detail on the case of cyclotron resonance (CR)[8], having in mind comparison with experiment in the next section. The contribution of the electrons to the dielectric constant, for right-hand polarization (which is active in CR) is obtained in the form

$$\varkappa(\omega) = 1 - \frac{\omega_p^2}{\omega(\omega - \omega_c - \mathscr{M}^0(\omega))}, \quad \omega_p^2 = \frac{4\pi n e^2}{m}; \tag{7.10}$$

here n is the electron concentration and $\mathscr{M}^0$ is constructed in accordance with type (2.3) for p = 0:

$$\mathscr{M}^0(\varepsilon) = \int \frac{d^3q}{(2\pi)^3} \frac{|\gamma(q)|^2}{\varepsilon - \omega_0 - E_0(-q_{||}) + i0}, \tag{7.11}$$

where

$$|\gamma(q)|^2 = \mathscr{F}(q) \frac{1}{2}(aq_\perp)^2 \exp\left\{-\frac{1}{2}(aq_\perp)^2\right\}. \tag{7.12}$$

If we represent $\mathscr{M}^0(\epsilon)$ in the form

$$\mathscr{M}^0(\varepsilon) = \Delta E(\varepsilon) - i\Gamma(\varepsilon), \tag{7.13}$$

then we can easily see that this is a shift and a broadening, calculated in second order perturbation theory, of the level n = 1, k = 1 with energy ϵ.

Formula (7.10) admits of a simple interpretation. It can be assumed that allowance for the interaction with the phonons reduces to taking the shift ΔE and the broadening Γ of the final level into account in the transition frequency $\omega_c = E_1(0) - E_0(0)$. The only cause of the peculiarity of the absorption is therefore the fact that ΔE and Γ depend strongly on the frequency near the threshold (Fig. 17), this being a reflection of the singularity in the density of states of the Landau electron near the bottom of the band.

An analysis of (7.10) shows that at $\omega_c < \omega_0$ there should be observed a CR peak shifted towards lower frequencies by an amount on the order of $\alpha\omega_0$ with width Γ' determined by unaccounted for scattering mechanisms (absorption of optical phonons, impurities, acoustic phonons) and with oscillator strength $f \approx 1$, and also a weak absorption peak above the threshold with an oscillator strength $f \sim \alpha$. In the resonant field $\omega_c = \omega_0$, two peaks of comparable intensity ($f \sim 1$) should be observed, one narrow below the threshold, of width Γ', and the other broad, asymmetrical, above the threshold, with width on the order of $\alpha^{2/3}\omega_0$. Both peaks are shifted relative to ω_0 by an amount on the order of $\alpha^{2/3}\omega_0$. At $\omega_c > \omega_0$, a CR peak should again be observed, with a shift towards higher frequencies and with a width on the

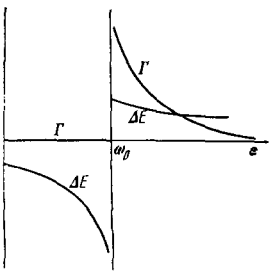

FIG. 17. Width and shift of the Landau level n = 1 as a result of electron-phonon interaction.

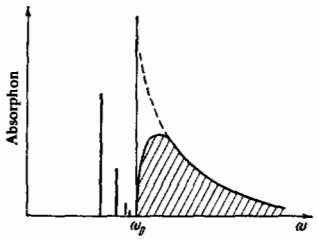

FIG. 18. Frequency dependence of the electron absorption in a magnetic field with allowance for bound states with phonons.

order of $\alpha\omega_0$ and with an oscillator strength $f \approx 1$, as well as a weak absorption peak below the threshold, with $f \approx \alpha$.

Further development of the CR theory for the resonance situation consists of taking the finite temperatures into account[59,60]. The splitting of the CR peak at $\omega_c = \omega_0$ becomes "washed out" if the temperature is $T \gtrsim \alpha^{2/3}\omega_0$. The influence of phonon dispersion on the character of the absorption was also considered[53].

A study of the second group of effects calls for a more detailed theory[61]. The absorption due to electron transitions from the bottom of the band $l = n = 0$ into bound states, i.e., for optical frequencies $\omega \approx \omega_0$, was calculated. The contribution of the electrons to the absorption (excluding the monotonic contribution of the free electrons) is expressed in terms of the scattering amplitude.

In the notation of Sec. (a) of this chapter, this expression is

$$\operatorname{Im}\varkappa^{\pm}(\omega) = \frac{\omega_c\omega_p^2}{\omega_0(\omega_0 \mp \omega_c)} \operatorname{Im}\{\lambda(\omega)\,\overline{\Phi} + \lambda^2(\omega)\,\overline{R}_{\pm 1}(\omega)\}, \qquad (7.14)$$

where

$$\overline{\Phi} = \int_0^\infty dt e^{-t}\Phi(t),$$
$$\overline{R}_{\pm 1}(\omega) = \int_0^\infty\int dt\,dt' e^{-(t+t')/2}(tt')^{1/2}[\Phi(t)\Phi(t')]^{1/2} R_{\pm 1}(\omega; t, t') \qquad (7.15)$$

The upper and lower signs pertain to right-hand and left-hand polarization of the light, respectively.

It is seen from (7.14) that, depending on the polarization of the light, the transition goes to bound states with $l = \pm 1$ from an initial state with $l = 0$. This means that the quantum number l describing the renormalized spectrum of the electron satisfies the same selection rules $\Delta l = \pm 1$ as the quantum number n describing the nonrenormalized spectrum. The selection rules are equally valid for positive and negative l.

The first term in the curly brackets of (7.14) corresponds to perturbation theory, i.e., to the single-phonon model. It yields the absorption in accordance with elementary theory of cyclotron-phonon resonance[62]. The second term can be easily analyzed by writing down the pole expansion of the resolvent.

The character of the absorption is illustrated by Fig. 18, where the dashed curve shows the absorption calculated without allowance for the bound states. The absorption below threshold ($\omega < \omega_0$) consists of a series of discrete lines concentrated in the region $|\omega - \omega_0| \sim W$, with rapidly decreasing intensity. The absorption above threshold ($\omega > \omega_0$) decreases like $(\omega - \omega_0)^{-1/2}$ far from the threshold, at $|\omega - \omega_0| \gg W$, and increases like $(\omega - \omega_0)^{1/2}$ near the threshold, at $|\omega - \omega_0| \ll W$. We see that allowance for the bound states modifies the absorption spectrum in analogy with the situation for the Mott exciton. The possibility of observing the fine structure of the spectrum is determined by the binding energy W and by the oscillator strength f_d in the discrete part of the spectrum relative to the strength f_c in the continuous part. Estimates of these quantities for the most important PO interaction[61] are given in Table II.

	$\omega_c \ll \omega_0$	$\omega_c \gg \omega_0$
$W \sim$	$\alpha^2\omega_0(\omega_c/\omega_0)^4$	$\alpha^2\omega_0$
$f_d \sim$	$\alpha^2(\omega_0/\omega_c)^5$	$\alpha^2(\omega_0/\omega_c)^2$
$f_c \sim$	$\alpha(\omega_0/\omega_c)$	

Observation of absorption in the region $\omega \approx \omega_0$ is made highly complicated by lattice effects. The observation of bound states occurring at the threshold of emission of a phonon with transition to the bottom of the band $n = 1$ (and not $n = 0$) is therefore more promising. Although these states lie near $\omega_c + \omega_0$, i.e., in the continuous spectrum, it can be shown[63] that if $\omega_c < \omega_0$, then their width is $\Gamma \sim \alpha\omega_0^2$, which is smaller than the binding energy $W \sim \alpha^2\omega_0$. The presence of these states should lead to a fine structure of the cyclotron-phonon resonance line at the frequency $\omega = \omega_c + \omega_0$. It is also possible to go outside the range of lattice effects by observing the fine structure of the combined-resonance line at the frequency $\omega = \omega_c + \omega_s$ (ω_s is the spin splitting).

The electron-phonon interaction exerts a highly unusual influence on Raman scattering, since a free electron with parabolic dispersion law in a magnetic field does not produce optical scattering with a frequency shift. This can be understood by considering the correspondence principle: such an electron is a harmonic oscillator and therefore does not mix the frequencies. This follows formally from the selection rules with respect to n and from the equidistant character of the Landau electron spectrum. The interaction with the phonons, as shown above, does not change the selection rules but makes the spectrum nonequidistant. As a result, scattering with a frequency shift $\overline{\omega} = \pm 2\omega_c$ becomes possible. Under magnetophonon resonance conditions, the theory predicts singularities that are in many respects analogous to the singularities of the CR[64,65].

d) Experiment—cyclotron and combined resonance. Experiments on cyclotron absorption under conditions of magnetophonon resonance $\omega_c = \omega_{LO}$ was carried out in 1967 on n-InSb independently by two groups: Dickey, Johnson, and Larsen[66] and Summers, Harper, and Smith[3]. Owing to the small electron mass ($m = 0.014m_0$), resonance in the infrared band ($\lambda \approx 50\ \mu$) is reached in not too strong fields (H = 34 kOe). The experiments were performed on pure samples at low temperatures (liquid nitrogen and lower).

Typical results, taken from[67], are shown in Fig. 19. The experimental points show the variation of the position of the CR line with changing magnetic field. The light circles correspond to transitions with spins antiparallel to the fields, and the dark one with spins parallel to fields. The straight lines are extrapolation

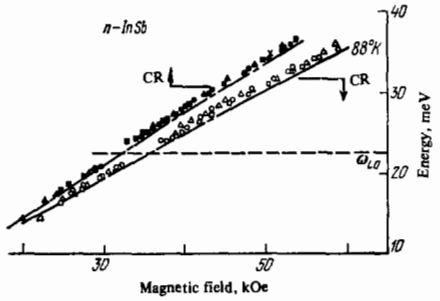

FIG. 19. Variation of cyclotron-absorption frequency with the magnetic field, according to [67].

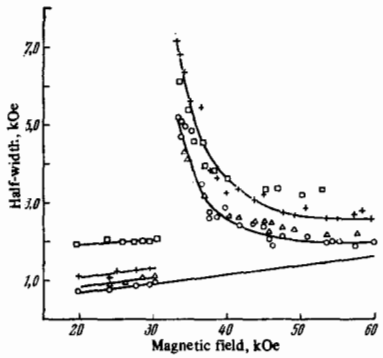

FIG. 20. Cyclotron-absorption line width [67].

from the side of weak fields, in which $\omega_c < \omega_{LO}$. It is seen in both cases that on going through the magnetophonon resonance $\omega_c = \omega_{LO}$ the position of the CR line, in accord with the theory, shifts jumpwise into the high-frequency region—the experimental points lie above the straight line. The CR frequency shift is $\Delta\omega_c \approx 0.5$ meV. If we assume $\alpha = 0.02$ and $\omega_{LO} = 24$ meV for n-InSb, then the theory yields $\Delta\omega_c \sim \alpha\omega_{LO} = 0.5$ meV; the agreement is perfectly satisfactory. Figure 20 shows the dependence of the width of the CR line on the field. We see that it increases sharply when resonance is approached from the direction of the strong fields, in full agreement with the behavior of Γ on Fig. 17. If we subtract from the width the monotonic background Γ' which is not connected with emission of optical phonons (extrapolation on Fig. 20), then the remaining width can be compared with the theoretical Γ. Such a comparison is shown in Fig. 21, where the dashed curve joins the experimental points and the solid lines correspond to the theory for two values of α. Recognizing that the theory does not take into account the thermal smearing ($T = 1$ meV, which is comparable with $\Gamma \approx 3$ kOe ≈ 2 meV), the agreement should be regarded as good.

The theoretically predicted splitting of the CR peak in resonant fields is not observed in the experiment, probably because the splitting $\alpha^{2/3}\omega_0 \approx 2$ meV is of the same order as the frequency region in which an important role is played by the lattice reflection ($\omega_{LO} - \omega_{TO} \approx 2$ meV) and by the lattice absorption ($|\omega - \omega_{TO}| < 5\%\ \omega_{TO} \approx 1$ meV).

The splitting of the peak in resonant fields can be observed in combined resonance[68], in which a transition from the $n = 0$ level to the $n = 1$ level with spin flip takes place. Since the LO-phonon emission takes place without spin flip, the threshold of the decay of the final state is $\omega_c = \omega_{LO}$, as in ordinary CR; yet the absorption takes place at the frequency $\omega = \omega_c + \omega_s$,

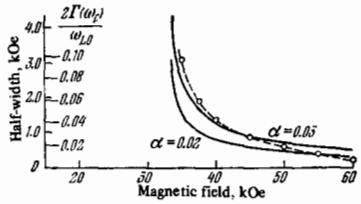

FIG. 21. Comparison of theory and experiment for the CR line width [67].

where ω_s is the spin splitting of the Landau level $n = 0$. In InSb at $H = 34$ kOe we have $\omega_s \approx 10$ meV, so that the electron absorption does not fall outside the region of the lattice reflection and absorption. The experimental results for n-InSb at 30°K[69] are shown in Fig. 22, which shows clearly not only the shift of the peak on going to the resonant field (on the order of 0.7 meV), but also the splitting of the peak in resonant fields (on the order of 1.5 meV, which agrees with the theoretical estimate $\alpha^{2/3}\omega_{LO} \approx 2$ MeV).

Similar effects were observed in impurity transitions in[70]. If the scattering by the phonons is accompanied by spin flip, resonant effects are possible when the phonon frequency ω_0 either coincides with the paramagnetic frequency ω_s[71] or with one of the combination frequencies $\omega_c \pm \omega_s$. Insofar as we know, no experiments were performed on Raman scattering under magnetophonon resonance conditions.

It is obvious that effects quite similar to those that occur near the threshold for the emission of one phonon can take place also near the threshold of emission of two and more phonons[32]. We take notice in this connection of the anomalies in the intensity of combined resonance in n-InSb, observed[73] at $H \approx 70$ kOe when the level $n = 1$ goes through the threshold of $2\omega_{LO}$. Another group of effects can be connected with participation of surface optical phonons. Thus, pinning was observed in p-InSb at the frequency ω_{TO}[74].

We shall show that the dispersion and the finite lifetime of the optical phonons do not influence these effects appreciably. The characteristic dimension of the electronic state is in this case the magnetic length, so that the phonon-energy scatter is $\Delta\omega_q \sim (m/\mu)\omega_c$ (see the end of Chap. 3), and the characteristic energy scale is $\alpha^{2/3}\omega_0$. The dispersion of the phonons and their width γ can therefore be disregarded if

$$\frac{\gamma}{\omega_0}, \frac{m}{\mu} \ll \alpha^{2/3}. \qquad (7.16)$$

This condition is satisfied in In-Sb, since $\gamma/\omega_0 \sim 10^{-2}$ $m/\mu \sim 10^{-3}$, and $\alpha^{2/3} \sim 10^{-1}$. The phonon dispersion was taken into account explicitly in[54].

An analysis of the experiments under conditions of magnetophonon resonance allows us to state that the influence of hybrid states on the optical effects has been reliably observed. In those cases when highly stretched pinning is observed, one can probably expect also the appearance of the bound states into which the hybrid states are transformed when the distance from resonance is increased.

Additional branches of the spectrum, which exist independently of the resonance, have not been observed so far, although they are possible. It is seen from (7.16) that the optimal fields are those with $\omega_c \sim \omega_0$, since W does not increase in stronger fields and the ratio f_d/d_c decreases. In n-InSb we have in this case

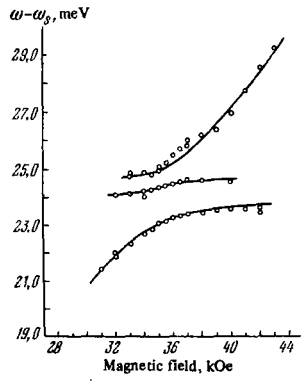

FIG. 22. Positions of absorption line in the combined-resonance spectrum in accordance with [69]. The presence of two pinnings is due to the participation of the localized and free electrons.

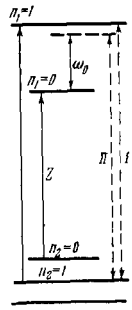

FIG. 23. Scheme of electron and hole Landau levels.

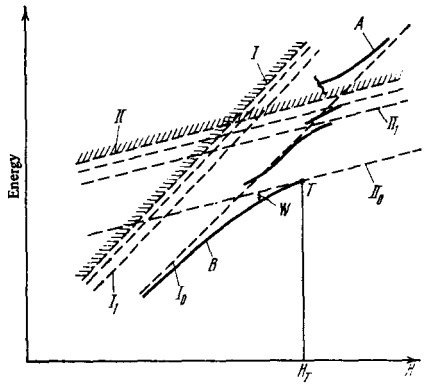

FIG. 24. Energy spectrum of electron and hole in a magnetic field with allowance for Coulomb attraction and electron-phonon interachon.

$W \approx 10^{-2}$ meV, which is beyond the experimental capabilities. More promising is CdTe, which has been used frequently of late to study magnetopolaron effects[75-77]. This material is attractive because it has a large coupling constant ($\alpha \approx 0.4$) at not too large a mass ($m = 0.096m_0$). Resonance is reached in a field $H = 180$ kOe, which is experimentally attainable. In fields of this order we have $W \sim \alpha^2\omega_{LO} \approx 3$ meV; the collision smearing in pure samples is $1/\tau \approx 0.2$ MeV. One can therefore expect the bound states to appear in optics, even if an unfavorable numerical factor decreases W by one order of magnitude.

8. EXCITON-PHONON COMPLEXES IN A MAGNETIC FIELD

The singularities that appear in the absorption spectra when the cyclotron frequency of the electrons is at resonance with the phonon frequency were first observed by Johnson and Larsen[2] in the spectrum of the intrinsic (interband) absorption in InSb. The physical picture is here much more complicated than in cyclotron (intraband) absorption, since a hole also takes part in the absorption process. To ignore the Coulomb interaction of the electron and the hole, as was done in[2] is, to say the least, unjustified, since the entire clearly pronounced structure in edge absorption is connected with exciton bands whose specific weight increases with increasing magnetic field[78]. In the investigation of polaron effects in interband absorption we therefore encounter a three-body problem (electron, hole, and phonon). Naturally, the problem can be solved only in limiting cases, only a few of which have been investigated so far.

The magnetoexciton is usually obtained under strong-field conditions, when

$$\omega_c,\ \omega_{c1},\ \omega_{c2} \gg R = \frac{me^4}{2\varkappa_\infty^2},\quad \frac{1}{m} = \frac{1}{m_1} + \frac{1}{m_2},\quad \omega_c = \frac{eH}{mc}, \qquad (8.1)$$

where the subscripts 1 and 2 refer to the electron and the hole. The carrier motion is quasi-one-dimensional; the transverse motion is determined by the magnetic field, and only the slow longitudinal motion is controlled by the Coulomb attraction. Therefore each pair of Landau bands n_1 and n_2 generates its own system of exciton levels E_S, $s = 0, 1, 2, \ldots$. Since the exciton is neutral on the whole, the total momentum P is an integral of the motion[79,80]; since we are interested in exciton absorption, we confine ourselves to states with $P = 0$. Assuming $L \equiv \ln(\omega_c/2R) \gg 1$, we have[78,81]

$$E_0 = -RL^2,\ E_s = -\frac{R}{s^2}\quad (s = 1, 2, \ldots). \qquad (8.2)$$

With increasing H, almost the entire absorption is concentrated in the band $s = 0$: its intensity increases like HL.

In the study of polaron effects it will be assumed that the holes do not interact with the phonons. This assumption can be fully justified only in the resonant situation $\omega_{c1} \approx \omega_0$, since the interaction of the holes with the phonons is nonresonant ($m_2 \neq m_1$) and is therefore insignificant. The assumption can be justified in the nonresonant situation, strictly speaking, only in nonpolar crystals, since the DO-interaction constants α_1 and α_2 are independent. In PO interactions, α_1 and α_2 are not fully independent, so that it would be necessary to take into account also the interaction of the hole with the phonons. This has not been done so far, however,

Figure 23 shows the scheme of electronic levels without allowance for the Coulomb interaction. We assume that the transitions between the edges of the hole and electron bands are allowed at $H = 0$. Then magnetooptical transitions $n_1 = n_2$, shown in Fig. 23 by the solid arrows, are allowed for isotropic bands. When the longitudinal motion of the particles is taken into account, the corresponding energies are continuous-absorption thresholds. We note that if the electron transition is accompanied by production of a phonon, then the selection rule $n_1 = n_2$ is lifted. The dashed segment I shows the energy of the phononless transition with pair production ($n_1 = 1$, $n_2 = 1$), while segment II shows the energy of production of a pair ($n_1 = 1$, $n_2 = 1$) with a phonon. The dependence of these thresholds on H is shown by lines I and II in Fig. 24; they coincide at $\omega_{c1} = \omega_0$. When the Coulomb interaction is taken into account, a series of exciton states $s = 0, 1, \ldots$, shown by the lines $I_0, I_1, \ldots, II_0, II_1, \ldots$, splits away from each threshold. The transition to the lower level I_0 should then predominate in the absorption spectrum; there should also be present weak transition to I_S ($s \neq 0$) and weak continuous absorption above I.

Further modification of the spectrum takes place when account is taken of the electron-phonon interaction. In analogy with Chap. 2, we can predict that this will

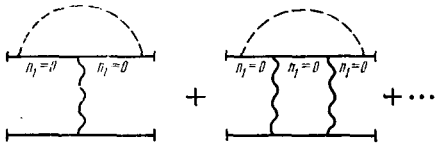

FIG. 25. System of basic diagrams for irreducible electron-hole vertex under resonance conditions (the wavy lines show the Coulomb interaction).

lead to pinnings near the crossing of levels belonging to the system I and system II. The levels constructed in this manner for the dominant transition are shown in Fig. 24 by thick lines. They correspond to magnetoexciton—phonon complexes. We note that the choice of the hole band $n_2 = 1$ is dictated exclusively by the selection rules for optically allowed transitions; a similar level scheme exists in principle also for $n_2 = 0$.

All these complexes are quasistationary, since they lie in the electron-hole continuum ($n_1 = 1$, $n_2 = 0$) and can decay with production of a fast electron and a fast hole. The rate of this decay, however, is small relative to the adiabatic parameter $R/\omega_0 \ll 1$, and we shall therefore neglect it. In this approximation, the complexes corresponding to the lower mode of the spectrum B (Fig. 24) can be regarded as stationary; W has the meaning of the binding energy relative to the detachment of a phonon from an exciton. The higher modes of the spectrum are nonetheless, however, modes relative to the production of the exciton ($n_1 = 0$, $n_2 = 1$) plus phonon pairs. We shall therefore consider henceforth, in accordance with[20,82], only the fundamental mode B and the states near its end point T.

In the study of polaron effects in the exciton spectrum, as already noted in Chap. 6, there arises the same question as in the polaron problem, that of the appearance of additional spectral modes describing bound states of particles and existing independently of the resonances. It was shown in[83] that under certain limitations on the parameters R, L, and m_2/m_1, these bound states of the electron, hole, and phonon actually exist. These states are also quasistationary with respect to the parameter R/ω_0.

a) Magnetophonon resonance. Under resonance conditions $\omega_{c1} \approx \omega_0$, as usual, we confine ourselves to the single-phonon approximation. This corresponds to retaining the first diagram of Fig. 4 in $\mathcal{M}$ and the sequence of diagrams of Fig. 25 in the electron-hole vertex. The main difference from Chap. 2 lies in the presence of internal degrees of freedom in the exciton. Therefore, instead of the algebraic equation (2.2) for the spectrum we obtain here an integro-differential equation for the Green's function $F(\omega \mid z, z')$ describing the longitudinal internal motion in an exciton with a momentum $P = 0$[82],

This equation is

$$[\varepsilon - \omega_{c1} - \omega_0 - \mathcal{H}_{P=0}^{n_1 n_2}(z)]F(z, z') - \int \mathcal{M}(\varepsilon \mid z, \bar{z})F(\bar{z}, z')\,d\bar{z} = \delta(z - z'), \quad (8.3)$$

where the mass operator is given by

$$\mathcal{M}(\varepsilon \mid z, z') = \int \frac{d^3q}{(2\pi)^3} |\gamma(\mathbf{q})|^2 (z \mid (\varepsilon - \mathcal{H}_{\mathbf{P}-\mathbf{q}}^{n_1 n_2})^{-1} \mid z') \times \exp\left[-i\frac{m_2}{M} q_z (z - z')\right], \quad (8.4)$$

$$\mathcal{H}_P^{n_1 n_2} = \frac{P_z^2}{2m} + \frac{P_x^2}{2M} + U_P^{n_1 n_2}(z); \quad (8.5)$$

$U_P^{n_1 n_2}(z)$ is the Coulomb energy averaged on the functions of the transverse motion of the free electron-hole pair with momentum P and Landau quantum numbers

FIG. 26. Dependence of the levels of the magnetoexciton + phonon complex on H when the Coulomb interaction is weaker than the electron-phonon interaction. The binding energy increases sharply in comparison with the hole-detachment energy W to the right of the resonance. (Lines 1 and 2 correspond to lines I and II of Fig. 24.)

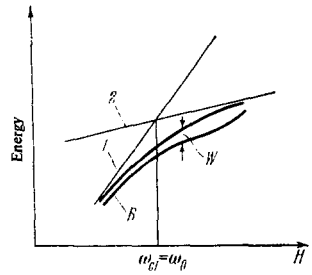

n_1 and n_2, while γ is defined by (7.12). The energy ϵ in (8.3) is reckoned from the straight line II of Fig. 24. The bound-state spectrum is determined by the poles F, and the absorption spectrum is determined by the function $F(\omega \mid z = 0, z' = 0)$.

Near the threshold, i.e., when the straight line II_0 is approached (see Fig. 24), $\mathcal{M}$ behaves in accordance with (2.5b). The spectrum is therefore similar to curve 2 of Fig. 2: it has an end point T at which it approaches the straight line II_0 tangentially. Consequently, according to Chap. 2, exciton plus phonon bound states are produced on curve B near T, and hybrid states are produced opposite the intersection of I_0 and II_0. Thus, the magnetoexciton spectrum differs greatly from the magnetopolaron spectrum in that it has an end point, which results from the fact that the transverse mass of the magnetoexciton $M_\perp$ is finite albeit large.

The limiting cases that can be investigated more completely, depending on the ratio of the Coulomb energy L^2R to the characteristic energy $(\alpha/2)^{2/3}\omega_0$ of the resonant electron-phonon interaction for the magnetopolaron (cf. Chap. 7). If $L^2R \gg (\alpha/2)^{2/3}\omega_0$[20,82], then we have at resonance

$$W \approx \alpha\omega_0 (\omega_0/2LR)^{1/2} (M/m_1)^{1/2}. \quad (8.6)$$

The effect is weaker here than in the magnetopolaron (on the order of α and not $\alpha^{2/3}$), but become stronger in comparison with the usual exciton, as a result of the factor $\omega_0/LR \gg 1$.

The absorption spectrum should consist of a narrow band corresponding to the appearance of a complex (curve B) and of a continuum corresponding to production of exciton plus phonon pairs; its maximum lies almost directly beyond the line II_0. As $H \to H_T$, the maximum of the background and the narrow band approach each other and coalesce, the intensity of the band decreasing continuously. At $H > H_T$ only the continuum is left, but its maximum also gravitates initially towards II_0. All this should produce a pinning picture—motion of the absorption maximum along II_0.

If $L^2R \ll (\alpha/2)^{2/3}\omega_0$[82], then it is more expedient to represent the level scheme in a somewhat different manner. In Fig. 26, the upper solid curve shows the energy of the magnetopolaron plus phonon complex, and the lower curve that of the magnetoexciton plus phonon complex. Therefore W has the meaning of the binding energy with respect to detachment of a hole. In the left part of the curve, this energy is close to L^2R, but after passing through resonance (after the intersection of 1 and 2) it begins to increase rapidly. Thus, under these conditions the electron-phonon interaction leads to a considerable enhancement of the effective attraction between the electron and the hole. On the section where W increases, the intensity of the absorption with formation of a complex (branch B) remains practically un-

changed. Subsequently W begins to decrease and the absorption decreases rapidly at the same time.

b) Additional modes of the spectrum. The question of the existence of additional branches of the spectrum in the three-body (electron, hole, and phonon) problem near the threshold for the production of a pair ($n_1 = 0$, $n_2 = 0$) and the phonon was also investigated[83]. The spectrum was obtained from the three-particle T matrix, for which it is possible to write an equation analogous to the two-particle equation (3.8). If we assume both the Coulomb and the polaron interactions to be weak, then the equation for the T matrix can be investigated by methods close to those described in Chap. 3, although the technical aspect of the problem becomes much more complicated. As a result, the problem of the spectrum of the T matrix can be reduced to the more lucid problem of the spectrum of the following Schrödinger equation:

$$\left[\frac{1}{2m_1}\frac{\partial^2}{\partial z_1^2}+\frac{1}{2m_2}\frac{\partial^2}{\partial z_2^2}+\varepsilon-V\delta(z_1)-U\delta(z_1-z_2)\right]\Psi(z_1, z_2)=0. \quad (8.7)$$

Here ϵ is the energy reckoned from the threshold; z_2 and z_1 are the longitudinal coordinates of the hole and of the electron that interacts with the immobile phonon at the point $z = 0$. The two potential terms describing the polaron and Coulomb interaction, respectively.

The potential V is determined by the eigenvalue λ^r of the polaron kernel $\Box$ (Chap. 7). If we put $U = 0$ and solve the equation with respect to z_1, then the eigenvalue will be the binding energy of the electron and phonon with $p = 0$, i.e.,

$$|\varepsilon| = W|_{U=0} = \frac{1}{2}m_1V^2 = \frac{\tilde{\alpha}^2\omega_0}{(\lambda^r)^2}. \quad (8.8)$$

Thus, each additional in the magnetopolaron spectrum has its own equation (8.6) with the appropriate value of V. If we put $V = 0$ and solve the equation with respect to $z_1 - z_2$, then the eigenvalue is the binding energy of an electron and a hole in the lower state, i.e.,

$$|\varepsilon| = W|_{V=0} = \frac{1}{2}mU^2 = RL^2. \quad (8.9)$$

Equation (8.7) can be easily investigated in various limiting cases, from which it is seen that at least one bound state of the three particles always exists (for each bound state of the electron plus phonon pair).

Equation (8.7) takes no account of two circumstances: 1) the possible decay of the bound state with transformation of the phonon energy into kinetic energy of the relative motion of the pair, which leads to a certain finite level width Γ; 2) the energy of the recoil of the transverse motion of the exciton, which can exist by virtue of the finite transverse exciton mass $M_\perp$ and therefore prevents the occurrence of bound states. Both effects can be taken into account in the equation for the T matrix by perturbation theory, and the smallness of the corresponding corrections in comparison with W yields a criterion for the existence of bound states of three particles. For example, at

$$R\tilde{L} \ll \alpha^2\omega_0 \ll R\tilde{L}^2, \quad \tilde{L} \equiv L\frac{m_1}{m_2} \gg 1 \quad (8.10)$$

we have

$$W \sim \frac{m_2}{m_1}\alpha^2\omega_0, \quad \Gamma \sim \frac{m_2}{m_1}\alpha^2\omega_0\left(\frac{RL^2}{\omega_0}\right)^{3/2}, \quad (8.11)$$

i.e., we have indeed $\Gamma \ll W$ relative to the adiabatic parameter RL^2/ω_0.

c) Experimental data. Figure 27 shows the experimental data[7] on interband magnetoabsorption in InSb, which have stimulated the development of the theory of resonant electron-phonon interaction. The curves show the positions of the maximum of individual bands as functions of the magnetic field. The general picture is quite similar to the scheme of Fig. 24. The pinning is clearly seen; the difference between the asymptotes (l_2 and l_3) for the upper and lower branches is undoubtedly due to the Coulomb interaction; it appears that the additional branches lying between 1 and 2 stem from the same source. The fact that the effect is entirely due to the electron-phonon interaction is clear also from the band Z (cf. Fig. 23), which experiences no noise whatever in this range of fields. One can assume that the pinning picture is just as clearly pronounced, owing to the large mass ratio $m_2/m_1 \sim 10$, and the higher quasistationary states are clearly seen because of the weak coupling $\alpha \approx 0.02$.

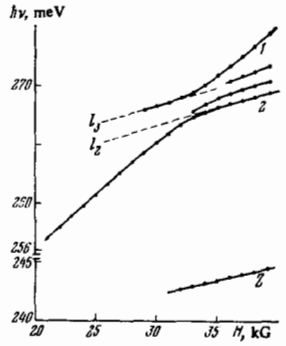

FIG. 27. Positions of peaks of intrinsic absorption of InSb, according to [7], in the region of magnetophonon $\omega_{cl} \approx \omega_0$. Band 2 can be set in correspondence with the ground state of the magnetoexciton + phonon complex (1 and 2 correspond to A and B in Fig. 24.)

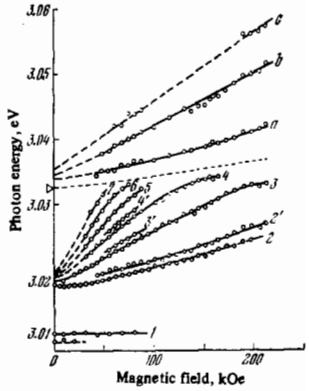

FIG. 28. Dependence of TlBr exciton-absorption peak frequency on H at 4.2° K (according to [49]). The light triangle corresponds to the energy $E_{exc} + \omega_0$, and the dashed line drawn from it is the pinning threshold.

A more complete comparison of theory with experiment is at present impossible for two reasons. First, there are no experimental data on the dependence of the absorption intensity in band 2 on the magnetic field, nor are there any data on the spectral distribution of the absorption beyond the asymptote l_2, where dissociation of the complexes should set in. In addition, in InSb we have $L \approx 3$, $L^2R \approx 0.6$ meV, and $(\alpha/2)^{2/3}\omega_0 \approx 0.8$ meV. Consequently, the logarithmic approximation is at the applicability limit, and in addition, $L^2R \sim (\alpha/2)^{2/3}\omega_0$, i.e., the theory can claim only a description of the quantitative tendencies.

Figure 28 shows analogous data for TlBr[49], which is a crystal with intermediate coupling ($\alpha \approx 2.5$). The bands 1—3 correspond to the successive terms of the lower exciton series, while bands 4—7 correspond to the excitons from the succeeding magnetic sub-bands. Here $\omega_0 \gg R \gtrsim \omega_c$, i.e., fields ~100 kG cannot be regarded as strong, and consequently the situation is intermediate between those considered in Chaps. 6 and

8. The pinning picture is very clearly pronounced. It is interesting that bands 4–7 have no continuation analogous to curve 1 of Fig. 27. It is natural to attribute this to the large width of the upper states, due to the intermediate coupling. In these experiments, there is one more interesting feature, noted but not explained in[49], namely, the pinning is observed not near the first threshold ($E_{1s} + \omega_0$) but near $E_{exc} + \omega_0$, where E_{exc} is the energy of the lower excited states. It is natural to explain this fact on the basis of the results of Chap. 6: the optically excited s-states should experience the strongest pinning in interaction with p-states. Consequently, the pinning should set in near $E_{2p} + \omega_0$, in full agreement with experiment.

Thus, exciton-phonon complexes were observed in the resonance situation for both weak and intermediate coupling. They have not yet been observed in a nonresonance situation.

9. CONCLUSION

Bound states with participation of optical phonons have two qualitative differences from ordinary bound states. The first is due to the fact that particles whose number is not conserved take part in them. Therefore such states are stable only because their real decay with vanishing of a phonon is forbidden by the conservation law (energy in the case of a localized electron, and energy-momentum for a free electron or exciton). The second difference is due to the absence of a simple conception of the character of the interaction in configuration space, where the electron-phonon interaction is essentially nonlocal. Thus, in particular, it is not obvious beforehand whether the interaction between the electron and the phonon is effectively attraction or repulsion.

It should be emphasized that the existence of bound states with optical-phonon participation has nothing in common with the well known intersections of the boson modes, first considered in the theory of optomechanical oscillations by Tolpygo[84] and by Huang[85], although many of the pictures (for example, Fig. 3) are quite similar[5]. For the resonance situation the difference between these phenomena can be explained, for example, in the following manner: For boson intersections, both resonant states are single-particle, whereas for the systems considered by us one of the states is single-particle and the other is two-particle. It is this which generates the difference in the results, namely the appearance of end points, of additional modes, etc.

The formation of complexes is determined by the competition between the kinetic energy of the particle with which the complex is bound and the energy of their interaction; the character of the complex and the energy scale of the structure of the spectrum therefore depend strongly on the degree of localization of the particle that takes part in the formation of the complex. When an electron and a phonon are bound, the effects are strongest if the electron is localized on an impurity center: the energy scale of the structure of the spectrum is of the order of $\alpha^{1/2}\omega_0$ at resonance and $\alpha\omega_0$ off resonance (we assume that $\alpha \ll 1$). For an electron in a magnetic field, which is "localized only across the field, the effects are weaker: $\alpha^{2/3}\omega_0$ at resonance and $\alpha^2\omega_0$ off resonance. If there is no magnetic field, then the bound states exist only in the case of strong coupling ($\alpha \gg 1$) and possibly also in the intermediate-coupling state. The exciton, being a neutral particle, is not "localized" by the magnetic field, so that there is no strong difference between the behavior of a magnetoexciton + phonon complex and that of an exciton + photon complex. However, a strong magnetic field increases the transverse mass of the magnetoexciton, bringing it close to that of the magnetopolaron. This contributes to the appearance of bound states with the phonon. Acting in the same direction is an increase in the ratio of the hole and electron masses in the ordinary exciton, bringing its properties closer to those of the impurity center.

The comparison of theory with experiment is still in the initial stage, and in many cases even the qualitative interpretation is not unambiguous. The only question where there is full qualitative and semiquantitative agreement is intraband absorption in n-InSb under conditions of magnetophonon resonance. For interband absorption under the same conditions, there is no doubt that the cause of the effect is correctly understood, but there is still no detailed interpretation of the spectrum. No bound states were sought under nonresonant conditions, although their observation in crystals that are more polar than InSb, for example in CdTe, is perfectly realistic. It can be assumed that such states should lead to a fine structure of the cyclotron-phonon resonance peaks.

There is no doubt that the bound states of a localized electron with an optical phonon (dielectric local vibrational modes) have been experimentally observed, including also in the nonresonant situation. Their comparison with the levels of the theoretical spectrum is, however, not fully clear.

In the case of an exciton without a magnetic field, there is practically no agreement between theory and experiment, and the nature of the singularities in the spectrum in the region of energies of the electron-hole continuum remains unclear, it being uncertain whether they are due to exciton plus phonon complexes or simply to interference effects.

The bound states should become manifest in most natural fashion in absorption experiments, as a result of interaction between the particles produced upon absorption of the photon (interaction in the final state). Naturally, the same bound states can be observed in principle also in hot luminescence, but this time as a result of interaction in the initial state. In luminescence they can be manifest in certain cases also as a result of interaction in the final state and it is precisely in this way that center + phonon bound states are observed in the vibrational satellites of the luminescence of impurity excitons.

There is no doubt that bound states with phonon participation can affect also other phenomena. For example, since phonons can become bound with different quasiparticles, these quasiparticles can in principle become bound to one another via a real phonon. This means that excited quasistationary bound states of quasiparticles can arise even if there are no bound states in the ground state. Arguments of this kind may turn out to be important for the interpretation of different optical and kinetic experiments. By way of another example we can point to the question of valley-orbit splitting in the exciton spectrum, which has been under discussion recently[87-89]. For the ground state of the exciton, such a splitting is obviously impossible because of translational symmetry. For the exciton plus phonon complex, how-

ever, which can have zero momentum (owing to the cancellation of the momenta of the two particles), such a splitting should arise and appear in the spectrum.

It should be borne in mind that the concrete systems considered in Chaps. 4—8 correspond to the traditional objects of the experimental papers. However, the approach developed in Chap. 3 is general, and it is possible to study on its basis also other systems, to the extent that experiments on these systems are performed. In connection with recent work on spatially-quantized electronic spectra of thin films and on surface phonons, it must be emphasized that in systems with smaller dimensionality the conditions for the formation of bound states with phonon participation should turn out to be particularly favorable in a number of cases.

[1)] The experimental data are analyzed in greater detail in [17].

[2)] For DO interactions, the integral for $\mathscr{M}^0$ diverges at large q, and this case will not be considered here.

[3)] The number of dielectric modes is limited by the phonon dispersion; its role in some cases was analyzed in [10, 32]. Using the remark made at the end of Chap. 3, we can easily indicate a criterion under which the dispersion can be neglected. Since the role of a is played here by the Bohr radius of the center, allowance for (5.12) yields $\alpha(\omega_0/R)^{3/2} \gg m/\mu$. In systems with a more complicated spectrum, the phonon dispersion can sometimes contribute to the formation of bound states [33].

[4)] A review of different effects that arise under conditions of magnetophonon resonance is given in [53].

[5)] A list of boson modes with participation of a longitudinal optical phonon is considered in the riview [86].

[1] J. Appel, Sol. State Phys. 21, 193 (1968).
[2] E. J. Johnson and D. M. Larsen, Phys. Rev. Lett. 16, 655 (1966).
[3] C. J. Summers, P. G. Harper, and S. D. Smith, Sol. State Comm. 5, 615 (1967).
[4] W. Y. Liang and A. D. Yoffe, Phys. Rev. Lett. 20, 59 (1968).
[5] A. Onton, P. Fisher, and A. K. Ramdas, ibid. 19, 781 (1967).
[6] L. D. Landau and E. M. Lifshitz, Kvantovaya mekhanika (Quantum Mechanics) Moscow, Fizmatgiz, 1963, Sec. 144 [Addison-Wesley, 1965].
[7] D. M. Larsen and E. J. Johnson, J. Phys. Soc. Japan Suppl. 21, 443 (1966).
[8] P. G. Harper, Proc. Phys. Soc. 92, 793 (1967).
[9] L. I. Korovin and S. T. Pavlov, Zh. Eksp. Teor. Fiz. 53, 1708 (1967) [Sov. Phys.-JETP 26, 979 (1968).
[10] Sh. M. Kogan and R. A. Suris, Zh. Eksp. Teor. Fiz. 50, 1279 (1966) [Sov. Phys.-JETP 23, 850 (1966)].
[11] Y. Toyozawa and J. Hermanson, Phys. Rev. Lett. 21, 1637 (1968).
[12] V. I. Mel'nikov and É. I. Rashba, ZhETF Pis Red. 10, 95, 359 (1969) [JETP Lett. 10, 60 (1969)].
[13] A. Yu. Matulis, Fiz. Tverd. Tela 14, 2987 (1972) [Sov. Phys.-Solid State 14, 2564 (1973)].
[14] I. B. Levinson, A. Yu. Matulis, and L. M. Shcherbakov, Zh. Eksp. Teor. Fiz. 60, 1097 (1971) [Sov. Phys.-JETP 33, 594 (1971).
[15] L. P. Pitaevskiĭ, Zh. Eksp. Teor. Fiz. 36, 1168 (1959) [Sov. Phys.-JETP 9, 830 (1959)].
[16] I. V. Levinson, ZhETF Pis. Red. 12, 496 (1970) [JETP Lett. 12, 347 (1970)].
[17] Y. B. Levinson and É. I. Rashba, Rept. Progr. Phys. 36, No. 12 (1973).
[18] É. I. Rashba and Y. B. Levinson, Proc. of the 11th Intern. Conference on the Physics of Semiconductors, Warsaw, 1972, p. 1197.
[19] G. Whitfield and R. Puff, Phys. Rev. A139, 338 (1965).
[20] V. I. Mel'nikov, É. I. Rashba, and V. M. Édel'shteĭn, ZhETF Pis. Red. 13, 269 (1971) [JETP Lett. 13, 192 (1971)].
[21] I. B. Levinson and A. Yu. Matulis, ibid. 11, 360 (1970) [JETP Lett. 11, 241 (1970)].
[22] I. B. Levinson, A. Yu. Matulis, and L. M. Shcherbakov, Zh. Eksp. Teor. Fiz. 61, 843 (1971) [Sov. Phys.-JETP 34, 449 (1972)].
[23] A. Suna, Phys. Rev. A135, 111 (1964).
[24] É. I. Rashba, ZhETF Pis. Red. 15, 577 (1972) [JETP Lett. 15, 411 (1972)].
[25] B. I. Kaplan and I. B. Levinson, Fiz. Tverd. Tela 14, 1412 (1972) [Sov. Phys.-Solid State 14, 1212 (1972)].
[26] D. D. Dunn, Phys. Rev. 166, 822 (1968).
[27] R. J. Heck and T. O. Woodruff, Phys. Rev. B3, 2056 (1971).
[28] S. I. Pekar, Zh. Eksp. Teor. Fiz. 16, 335, 341 (1946).
[29] L. D. Landau and S. I. Pekar, Zh. Eksp. Teor. Fiz. 18, 419 (1948).
[30] a) N. N. Bogolyubov, Ukr. Mat. Zh. 2, 3 (1950); b) S. V. Tyablikov, Zh. Eksp. Teor. Fiz. 21, 377 (1951).
[31] S. I. Pekar, Issledovaniya po elektronnoĭ teorii kristallov (Research on the Electron Theory of Metals), Gostekhizdat, 1951.
[32] S. Rodriguez and T. D. Schultz, Phys. Rev. 178, 1252 (1969).
[33] V. Fedosejev, Preprint FAI-5 (1970).
[34] É. I. Rashba, Izv. AN SSSR, ser. fiz. 37, 619 (1973).
[35] H. J. Hrostowski and R. H. Kaiser, J. Phys. Chem. Sol. 4, 148 (1958).
[36] B. T. Ahlburn and A. K. Ramdas, Phys. Rev. 167, 717 (1968).
[37] a) P. J. Dean, D. D. Manchon, Jr., and J. J. Hopfield, Phys. Rev. Lett. 25, 1027 (1970); b) D. D. Manchon, Jr., P. J. Dean, Proc. of the 10th Intern. Conference on the Physics of Semiconductors, Cambridge, Mass., 1970, p. 760.
[38] D. C. Reynolds, C. W. Litton, and T. C. Collins, Phys. Rev. B4, 1868 (1971).
[39] C. H. Henry and J. J. Hopfield, ibid. B6, 2233 (1972).
[40] J. C. Hermanson, ibid. B2, 5043 (1970).
[41] L. Kalok and J. Treusch. Phys. Stat. Sol. b52, K125 (1972).
[42] W. C. Walker, D. M. Roessler, and E. Loh, Phys. Rev. Lett. 20, 847 (1968).
[43] R. C. Whited and W. C. Walker, ibid. 22, 1428 (1969).
[44] R. C. Brandt and F. C. Brown, Phys. Rev. 181, 1241 (1969).
[45] H. Kanzaki, S. Sakuragi, and S. Ozawa, J. Phys. Soc. Japan 24, 652 (1967).
[46] H. Kanzaki and S. Sakuragi, ibid. 24, 1184 (1968).
[47] J. Sak, Phys. Rev. Lett. 25, 1654 (1970), p. 525.
[48] R. Z. Bachrach and F. C. Brown, Phys. Rev. Lett. 21, 685 (1968); Phys. Rev. B1, 818 (1970).
[49] S. Kurita and K. Kobayashi, J. Phys. Soc. Japan 26, 1557 (1969); 28, 1096, 1097 (1970); 30, 1645 (1971).
[50] J. Dillinger, C, Konak, V. Prosser, J. Sak, and M. Zvára, Phys. Stat. Sol. 29, 707 (1968).
[51] U. Fano, Phys. Rev. 124, 1866 (1961).
[52] Y. Toyozawa, Proc. of the 3rd Intern. Conference on Photoconductivity, L., Pergamon Press, 1971, p. 151.
[53] P. G. Harper, J. W. Hodby, and R. A. Stradling, Rept. Progr. Phys. 36, 1 (1973).
[54] L. I. Korovin and S. T. Pavlov, Zh. Eksp. Teor. Fiz. 55, 349 (1968) [Sov. Phys.-JETP 28, 183 (1969)].
[55] T. Holstein, Ann. Phys. (N.Y.) 29, 410 (1964); L. Dworin, Phys. Rev. A140, 1689 (1965).
[56] I. B. Levinson, A. Yu. Matulis, and L. M. Shcherbakov,

Zh. Eksp. Teor. Fiz. 60, 859 (1971) [Sov. Phys.-JETP 33, 464 (1971)].
[57] I. B. Levinson and É. I. Rashba, Zh. Eksp. Teor. Fiz. 62, 1502 (1972) [Sov. Phys.-JETP 35, 788 (1972)].
[58] K. L. Ngai and E. J. Johnson, Phys. Rev. Lett. 29, 1607 (1972).
[59] M. Nakayama, J. Phys. Soc. Japan 27, 636 (1969).
[60] L. I. Korovin, Zh. Eksp. Teor. Fiz. 58, 1995 (1970) [Sov. Phys.-JETP 31, 1075 (1970)]; A. A. Klyukanov and E. P. Pokatilov, Zh. Eksp. Teor. Fiz. 60, 1878 (1971) [Sov. Phys.-JETP 33, 1015 (1971)].
[61] B. I. Kaplan and I. B. Levinson, Fiz. Tverd. Tela 14, 1663 (1972) [Sov. Phys.-Solid State 14, 1434 (1972)].
[62] F. G. Bass and I. B. Levinson, Zh. Eksp. Teor. Fiz. 49, 914 (1965) [Sov. Phys.-JETP 22, 635 (1966)].
[63] R. Bakanas, I. B. Levinson, and A. Yu. Matulis, Zh. Eksp. Teor. Fiz. 64, 1065 (1973) [Sov. Phys.-JETP 37, 541 (1973)].
[64] P. G. Harper, Phys. Rev. 178, 1229 (1969).
[65] K. L. Ngai, ibid. B3, 1303 (1971).
[66] D. H. Dickey, E. J. Johnson, and D. M. Larsen, Phys. Rev. Lett. 18, 599 (1967).
[67] C. J. Summers, R. B. Dennis, B. S. Wherrett, P. G. Harper, and S. D. Smith, Phys. Rev. 170, 755 (1968).
[68] E. I. Rashba, Usp. Fiz. Nauk 84, 557 (1964) [Sov. Phys.-Usp. 7, 823 (1965)].
[69] B. D. McCombe and R. Kaplan, Phys. Rev. Lett. 21, 756 (1968).
[70] R. Kaplan and R. F. Wallis, ibid. 20, 1499.
[71] L. I. Korovin and S. T. Pavlov, ZhETF Pis. Red. 6, 970 (1967) [JETP Lett. 6, 383 (1967)].
[72] L. I. Korovin, Fiz. Tverd. Tela 11, 508 (1969) [Sov. Phys.-Solid State 11, 404 (1969)].
[73] B. D. McCombe, S. G. Bishop, and R. Kaplan, Proc. of the 9th Intern. Conference on the Physics of Semiconductors, Moscow, 1968, p. 301.
[74] R. Kaplan, K. L. Ngai, and B. W. Henvis, Phys. Rev. Lett. 28, 1044 (1972).
[75] J. Waldman, D. M. Larsen, P. E. Tannenwald, C. C. Bradley, D. R. Cohn, and B. Lax, ibid. 23, 1033 (1969).
[76] P. G. Harper, S. D. Smith, M. Allegrini Arimondo, R. B. Dennis, and B. S. Wherrett, p. 166.
[77] D. R. Cohn, D. M. Larsen, and B. Lax, Sol. State Comm. 8, 1707 (1970); Phys. Rev. B6, 1367 (1972).
[78] R. J. Elliott and R. Loudon, J. Phys. Chem. Sol. 15, 196 (1960).
[79] R. Knox, Theory of Excitons, Suppl. No. 5, Solid State Physics (Seitz and Turnbull, eds.), Academic, 1963.
[80] L. P. Gor'kov and I. E. Dzyaloshinskiĭ, Zh. Eksp. Teor. Fiz. 53, 717 (1967) [Sov. Phys.-JETP 26, 449 (1968)].
[81] H. Hasegawa and R. E. Howard, J. Phys. Chem. Sol. 21, 179 (1961).
[82] É. I. Rashba and V. M. Édel'shteĭn, Zh. Eksp. Teor. Fiz. 61, 2580 (1971) [Sov. Phys.-JETP 34, 1379 (1972)].
[83] I. B. Levinson, ZhETF Pis. Red. 15, 574 (1972) [JETP Lett. 15, 409 (1972)].
[84] K. B. Tolpygo, Zh. Eksp. Teor. Fiz. 20, 497 (1950).
[85] K. Huang, Proc. Roy. Soc. A208, 352 (1951).
[86] E. D. Palik and J. K. Furdyna, Rept. Progr. Phys. 33, 1193 (1970).
[87] G. Ascarelli, Phys. Rev. 179, 797 (1969); B3, 1498 (1971).
[88] K. L. Shaklee and R. E. Nahory, Phys. Rev. Lett. 24, 942 (1970).
[89] P. J. Dean, Y. Jafet, and J. R. Haynes, Phys. Rev. 184, 837 (1969); B1, 4193 (1970) (E).
Translated by J. G. Adashko